Carbon Letters (2022) 32:1603–1629
https://doi.org/10.1007/s42823-022-00359-1

Online ISSN 2233-4998
Print ISSN 1976-4251

REVIEW

Carbon nanodots: recent advances in synthesis and applications

Dheeraj Singh Chauhan[1,2] · M. A. Quraishi[3] · Chandrabhan Verma[3]

Received: 15 March 2022 / Revised: 16 May 2022 / Accepted: 16 May 2022 / Published online: 5 August 2022

Abstract

Due to their fascinating properties, there is a rise in the critical consideration of carbon-based nanomaterials in a plethora of applications. Carbon nanomaterials, such as nanotubes, graphene, fullerenes, and nanodiamonds, have broad applicability and potential research prospects. In the past few years, the developments and consumption of still smaller nanomaterials, namely graphene quantum dots and carbon nanodots or carbon dots (CDs) have been explored. Since carbon as a component exhibits insignificant cytotoxicity and remarkable biocompatibility, CDs have found a wide scope of potential applications. Owing to their fascinating aspects, such as small size, biocompatibility, low toxic nature, environment-friendliness, cost-effectiveness, ease of chemical functionalization, derivatization and surface modification, and photoluminescence tenability, CDs have been widely acknowledged. CDs have found major prospects in the areas of catalysis, sensors, and optical and bio-related applications. CDs are generally synthesized by employing techniques of pyrolysis, laser ablation, arc discharge, electrochemical method; hydrothermal and solvothermal techniques; and microwave and ultrasonic irradiations. This review article presents a brief account of the major properties of CDs, and applications, with particular emphasis on the green and environment-friendly synthesis methodologies. An overview of the microwave and ultrasound irradiation-induced syntheses for the preparation of CDs is presented in the light of green chemistry principles. In addition, some of the green and environmentally benign precursors for the production of CDs are outlined. The most recent work on CDs is included in this review article.

Keywords Carbon dots · Green chemistry · Nonconventional heating · Corrosion inhibitors · Sustainable developments

Abbreviations

SWCNT	Single-walled carbon nanotubes
MWCNT	Multi-walled carbon nanotubes
GO	Graphene oxide
GQDs	Graphene quantum dots
CDs	Carbon nanodots
PL	Photoluminescence
LED	Light-emitting diode
EL	Electroluminescence
TEM	Transmission electron microscopy
HRTEM	High-resolution transmission electron microscopy
XPS	X-ray photoelectron spectroscopy
EDPL	Excitation-dependent photoluminescence
EIPL	Excitation-independent photoluminescence
SDPL	Size-dependent photoluminescence
QY	Quantum yield
MW	Microwave
US	Ultrasound
HER	Hydrogen evolution reaction
OER	Oxygen evolution reaction
ORR	Oxygen reduction reaction
CO_2RR	Carbon dioxide reduction reaction
MBC	Minimum inhibitory concentration
ROS	Reactive oxygen species
PTT	Photothermal therapy
DFT	Density functional theory
MD	Molecular dynamics simulations

✉ M. A. Quraishi
maquraishi.apc@itbhu.ac.in

[1] Modern National Chemicals, Second Industrial City, Dammam 31421, Saudi Arabia

[2] Center of Research Excellence in Corrosion, Research Institute, King Fahd University of Petroleum and Minerals, Dhahran 31261, Saudi Arabia

[3] Interdisciplinary Research Center for Advanced Materials, King Fahd University of Petroleum and Minerals, Dhahran 31261, Saudi Arabia

1 Introduction

Over the years, carbon-based nanomaterials have found applications in a plethora of areas. The major application is in single and multi-walled carbon nanotubes (SWCNT, MWCNT), which can be classified into one-dimensional materials. Graphene and graphene oxide (GO), graphene quantum dots (GQDs), etc. come in the two-dimensional category, whereas fullerene, nanodiamonds, and carbon dots (CDs) can be termed as zero-dimensional [1–3]. Figure 1 shows the different forms of carbon nanoallotropes [2, 4]. Carbon nanodots (CDs) are carbon nanoparticles having a size in the dimensions of < 10 nm [5–7], are quasi-spherical, and are well dispersed [5, 8]. CDs, in general, comprise carbon skeleton besides other primary elements such as oxygen and hydrogen in varying ratios. CDs mostly exist in amorphous quasi-spherical shapes containing both sp^2 and sp^3 hybridized carbon atoms having a size < 10 nm [6].

In recent years, owing to their remarkable properties, such as low toxicity, high biocompatibility, nanoscale size, ease of chemical functionalization, and tunability of photoluminescence, CDs have been widely explored. The major applications are in catalysis, sensors, optical devices, and bioimaging [5, 9, 10]. CDs have been synthesized using both the top-down and the bottom-up methods depending upon the required application [6, 11]. The latter is the preferred one because of the large-scale and low-cost synthesis. Due to the stringent environmental regulation, nowadays, the greenness and sustainability of nanomaterials are major requirements. This is to avoid the discharge of any toxic/harmful effluent to the soil/aquatic life, leading to possible contamination/environmental pollution.

Several research articles have covered the chemical synthesis methodologies of CDs and their wide applicability. This article presents a brief account of the various synthesis strategies of CDs and their application. The important properties of the CDs are outlined and the biocompatible nature is highlighted. The focus is on the green and environmentally friendly synthesis of CDs with ease of preparation, scalability, and green nature. Accordingly, some of the modern synthetic techniques are reviewed for the preparation of CDs with desirable properties. Some

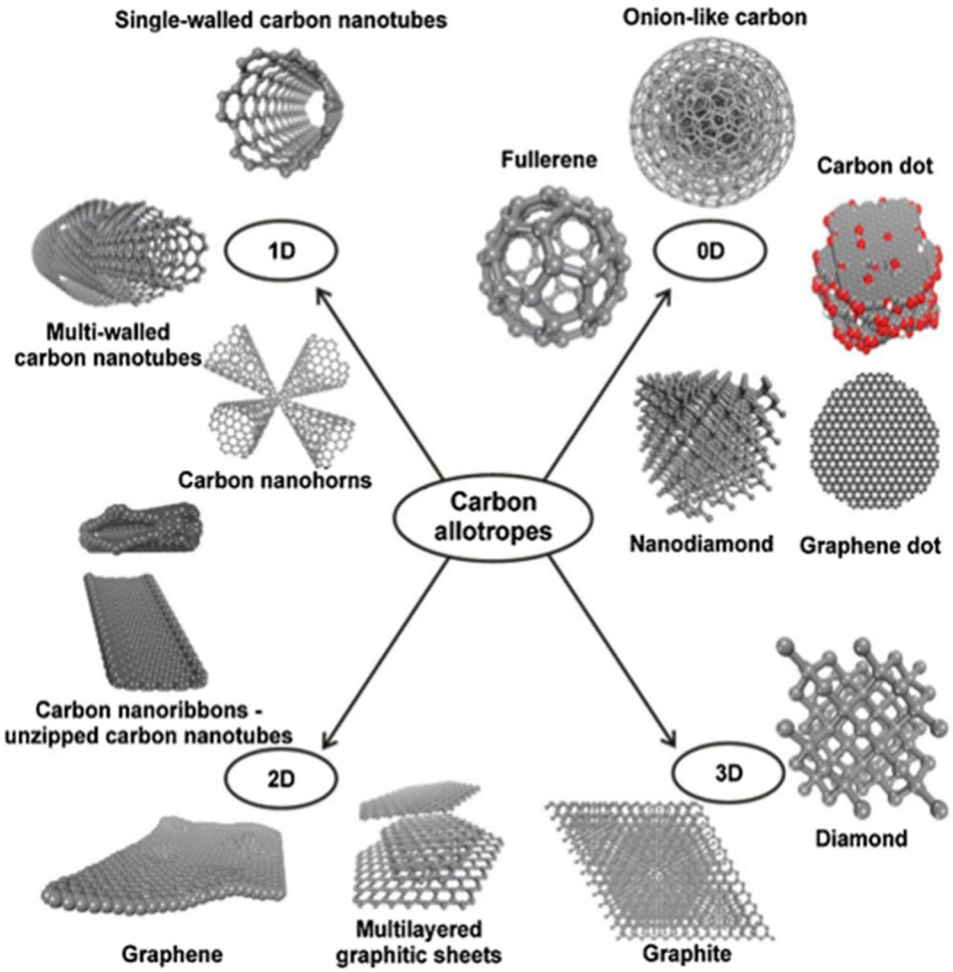

Fig. 1 Nanoallotropes of carbon [2, 4]

of the greener precursors of CDs are outlined, and a brief account on the applications of the CDs is presented. The scope of further research in this area is outlined.

2 Green synthesis of CDs

2.1 Top-down and bottom-up approaches

Depending upon the requirement for the target application, various synthetic strategies have been explored for the preparation of CDs. Figure 2a shows the general mechanism for the preparation of CDs. The different preparation

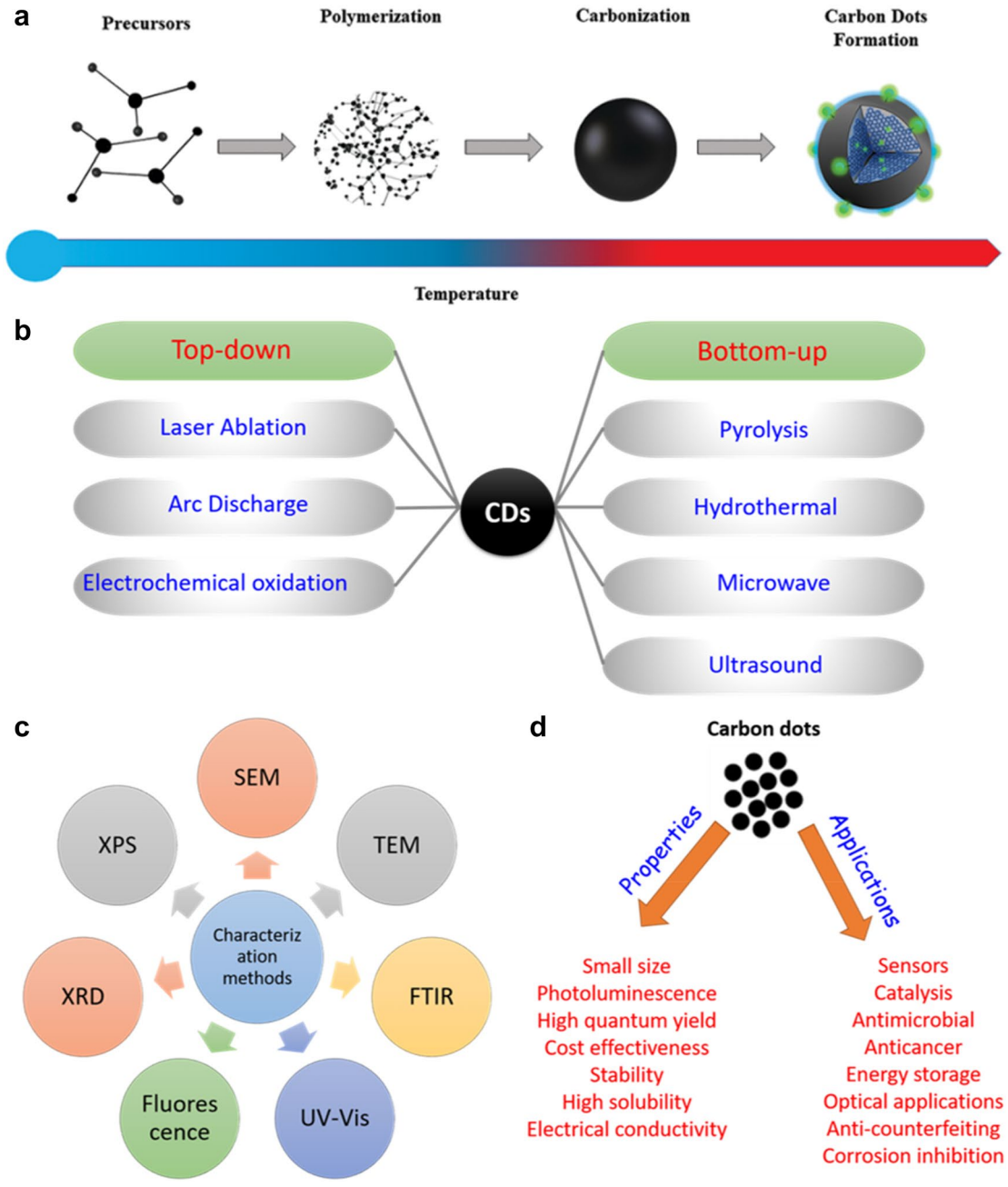

Fig. 2 **a** General mechanism for the preparation of CDs [12]; **b** top-down and bottom-up methods for the preparation of CDs; **c** major techniques used for the structural characterization of CDs; and **d** properties and applications of CDs

methods can be broadly categorized into the top-down and the bottom-up approaches, as shown in Fig. 2b. Chemical oxidation, mechanical grinding of activated carbon to get the nanoscale precursor (e.g., nanodiamond, carbon black, graphite, CNTs, ash), discharge, laser ablation, electrochemical preparation, etc., are the major top-down methods [3, 9, 10]. The bottom-up method describes the production of the nanomaterials using small molecules as precursors. These involve pyrolysis, microwave/ultrasonic irradiation, hydrothermal/solvothermal preparation, etc. The choice of the synthesis route stems from the following goals: (i) simplicity and reproducibility of the method, (ii) achieving high yield or scalability of the method, (iii) minimizing waste production, (iv) cost-effectiveness, and (v) optical properties. Figure 2c shows the major techniques used for the characterization of CDs. Some of the major properties and applications of the CDs are outlined in Fig. 2d.

2.2 Green synthetic methods of CDs

Green chemistry is the branch of science dealing with environmentally benign synthesis techniques, using safer solvents or solventless synthesis, minimizing waste production, use of enzymes, biocatalysts, etc. [13]. In this connection, herein, we present the microwave- (MW) and ultrasonication (US)-assisted methods for the preparation of CDs. Conventional organic synthesis methods require a long time for the organic synthesis to complete; therefore, these methods are considered inefficient and slower. Further, these methods offer poor selectivity and lower yields of the desired products. On the other hand, using the non-conventional methods of microwave and ultrasonic irradiations [12, 14, 15], the synthesis can be completed within a fraction of minutes and with a high product yield. These methods offer advantages of greater temperature homogeneity, uniform heating, reduced generation of waste, higher reaction rate and consquently low synthesis time, low operating cost, and high purity. Therefore, these techniques are considered environmentally benign and green methods. Almost all kinds of organic transformations have been reported using microwave and ultrasonic irradiations.

For the preparation of CDs, hydrothermal and solvothermal techniques are generally preferred. However, employing the MW and US methods, the synthesis time could be reduced from several hours to a few minutes [12, 16–18]. In addition, homogeneous heating during the MW irradiation method ensures the formation of uniform size CDs [19]. The use of template synthesis can provide good monodispersity and controlled size during CD preparation. The template synthesis methods can be facilitated using MW and US methods. Careful selection of MW/US parameters can provide a control over the size and morphology of nanoparticles even in the absence of any template [20]. Further, compared to the solvothermal method that employs non-aqueous solvents, the MW and US techniques can be carried out quite easily in aqueous media, thereby avoiding the use of toxic solvents. In addition, during the MW and US methods, visual changes and temperature profiles in the synthesis vessels can be easily followed and directly recorded, which is not possible for the hydrothermal method. Among MW and US techniques, the basic working principle is quite different and both techniques have their own merits as discussed below. Various kinds of catalytic reaction schemes can be further tuned by optimizing the MW and US parameters.

3 Significance of green synthetic methods for the preparation of CDs

3.1 MW irradiation

Conventional organic synthesis is slower, and the healing process can lead to the development of a temperature gradient within the sample. Besides, local overheating can lead to the decomposition of the desired product, substrate, and the used reagents. A domestic microwave (MW) is a common household appliance that is very commonly adopted for the cooking/re-heating of food items. This technique has also been reported successfully for numerous organic syntheses, preparation of nanomaterials, and solid-state science [21]. The MW region in the electromagnetic spectrum exists between the infrared and radio waves. Microwaves operate within wavelengths of 1 mm to 1 m, corresponding to frequencies between 0.3 and 300 GHz. MW radar and telecommunications systems occupy several band frequencies in this region. Thus, to avoid the disturbance from these, the MW apparatus for domestic and industrial purposes works at a frequency of 2.45 GHz. In the past few years, several reports have come up in the literature on the application of the MW method for the synthesis of nanomaterials [22–24]. The working principle of the MW reactors is based on dipolar polarization and ionic conduction [25, 26]. MW-induced synthesis offers the acceleration of organic reactions under selectivity of the resulting products by a careful selection of MW parameters [24, 27–29]. This offers considerable benefits over the conventional synthesis, such as quicker heating rates and greater thermal homogeneity.

The uniform heating of the reaction vessel in the MW method avoids the formation of heating gradients, which are common in the conventional hot plate and reflux methods [26, 30]. Thus, the MW method allows the development of uniform-sized nanomaterials [12]. Further, the choice of aqueous or suitable non-aqueous methods allows efficient hydrothermal/solvothermal synthesis. By modifying the conditions, viz., the MW power, synthesis time, and stirring

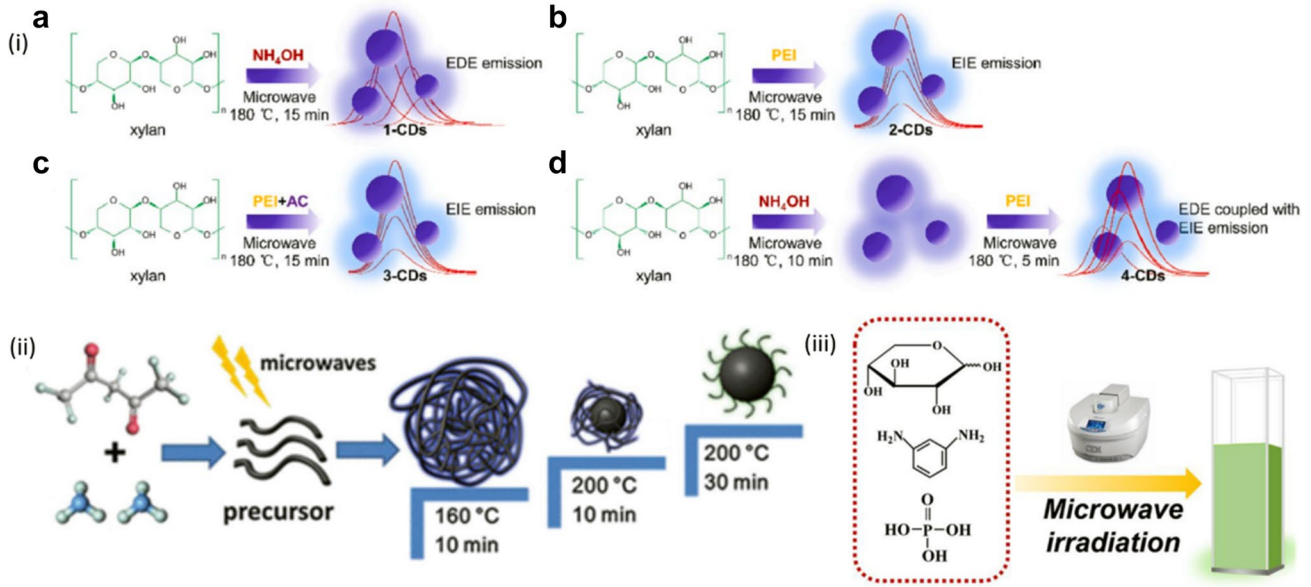

Fig. 3 Schematic of microwave-assisted synthesis of CDs using precursors: **a** xylan, NH_4OH, and PEI, to produce CDs having variable PL behavior [31]; **b** L-cysteine having N, S, doping, and variable sizes [32]; and **c** xylose [33]

speed (mechanical or magnetic), the desired shapes and sizes of nanomaterials can be obtained. Due to these benefits, the MW synthesis is a widely recognized green chemistry technique. Figure 3a–c shows the synthesis of CDs using xylan [31], L-cysteine [32], and xylose [33] as precursors following the MW technique. It has been observed that with an increase in MW reaction time, the UV–visible absorption peak at ~ 260 nm of the resulting CDs shifted to shorter wavelengths (4 min, 265.5 nm to 14 min, 253.5 nm) [34]. The authors have also noted that the QY of the CDs at first increased with an increase in the MW time and then decreased significantly [32]. In another report, the authors have noted that upon decreasing the MW reaction temperature, the QY is lowered. The FTIR spectra of the CDs prepared using xylan as discussed above using NH_4OH and PEI as precursors are shown in Fig. 4. In the following section, we present some examples from the literature on the application of MW method for the preparation of CDs.

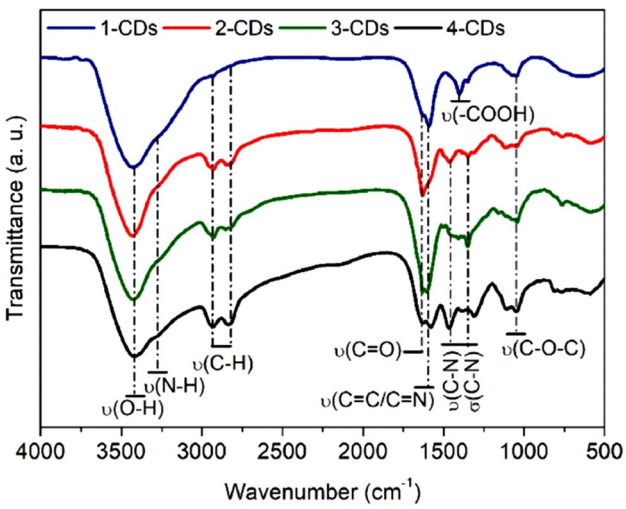

Fig. 4 FTIR spectra of CDs prepared from xylan following MW irradiation using different N-doping agents [31]

3.2 US irradiation

Ultrasound waves act as an alternative source of energy and have garnered significant interest in the area of green chemistry. The high-frequency ultrasonic (US) waves (20 kHz–10 MHz) induce a series of compression/rarefaction cycles through a solvent medium through which they are passed. This leads to the cavitation phenomenon in which bubbles form and collapse rapidly and provide energy to carry out the US-based reactions [21]. The creation of localized extremes of high temperature and pressure (hot spots) around/inside the cavitation bubbles not only destroys them, but also activates the reacting molecules of organic reagents [35]. Besides, micro jet streams and shock waves arising due to cavitation facilitate the mass transfer and dispersion of molecules in the medium [36]. Figure 5a–c shows the schematic of CDs synthesis employing the US method using gelatin hydrolysate [37], D-fructose [38], and crab shells [39] as precursors and its application in bioimaging, anti-counterfeiting, and heavy metal detection.

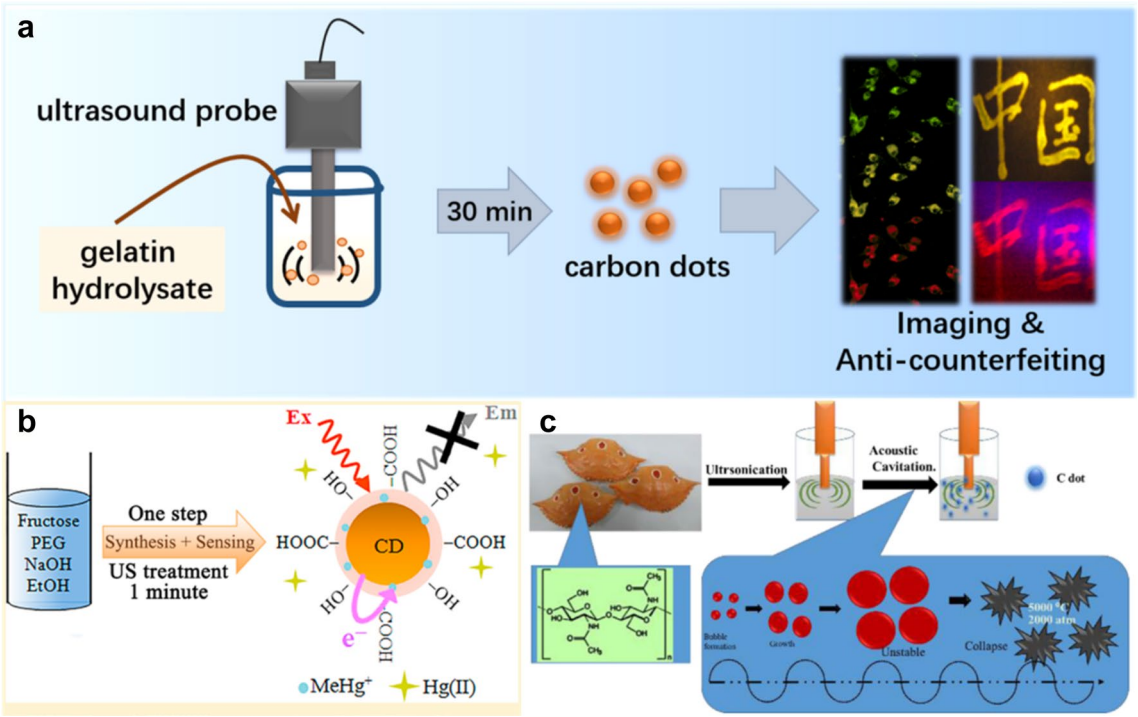

Fig. 5 Schematic of ultrasound-assisted preparation of CDs using precursors: **a** gelatin hydrolysate [37] and application in bioimaging and anti-counterfeiting; **b** D-fructose [38] and application in methylmercury detection; **c** crab shells [39], and application in the imaging of cancer cells

Ultrasonic (US) cleaner bath is the simplest ultrasonic processor commonly used for cleaning of artificial dentures, jewelry, and electrodes, and also for some organic synthesis in the laboratories. The US probe processor, on the other hand, is useful for dedicated application in organic chemistry, nanomaterial preparation, and other scientific purposes [14, 18, 36, 40, 41]. The probe processor comes with varying sizes of probes having radii generally varying from 3 to 10 mm. The major difference between the US cleaner and the US probe processor is that in the former, a reaction vessel is inserted into the water. In contrast, in the latter, the probe is directly inserted into the reaction vessel. The probe processor is more sophisticated and is of significantly greater power in comparison to the ultrasonic cleaner bath. This leads to more effective US action, and the probe instrument is dedicated to the specialized application. The synthesis procedure can be further modulated by adjusting the solvent, power, pulse period, energy, frequency, amplitude, sonication time, temperature, precursors, and catalysts. It has been noted that prolonged US treatment (6 h) results in the formation of heterogeneous nanoparticles [18]. In such conditions, the initially synthesized nanoparticles could behave as seeds that can promote the synthesis of greater-sized nanoparticles. However, the exact particle size will also be influenced by the size of the smaller-size particles and the concentration of the precursors. In general, for the preparation of CDs, a sonication time of 90–120 min is required. On the other hand, the sonication time also considerably influences the fluorescence intensity of the formed CDs. It has also been observed that the yield of CDs increases with sonication time and temperature [17]. In the following section, we have presented some examples from the literature on the application of the US technique for the preparation of CDs.

4 Importance of green precursors for CDs synthesis

In the above sections, we have outlined the application of MW and US techniques for the preparation of CDs using various types of precursor chemicals. In addition to the above, there are several precursors that can be categorized as green and environmentally benign, and their application in the synthesis of CDs is under the provisos of green chemistry principles of environmentally benign and low-toxicity reagents, renewable raw materials, and minimizing waste production (Table S1 in the Supporting Information) [13, 42]. The major categories of such

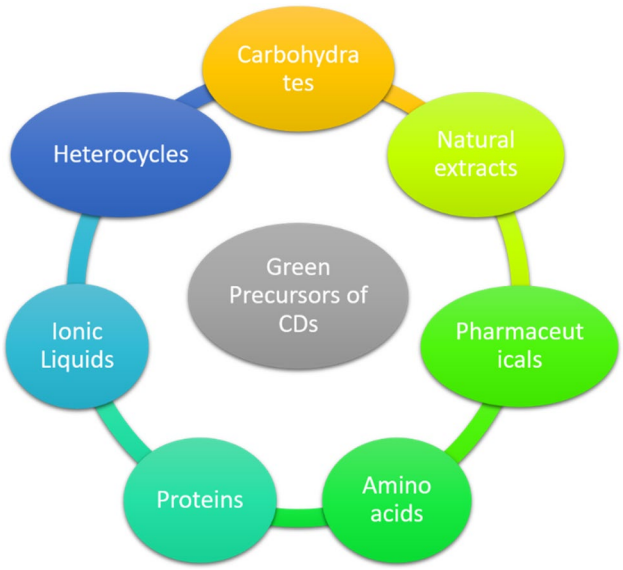

Fig. 6 Some of the green precursors used for the preparation of CDs

kinds of precursors include the extracts derived from naturally occurring plants [43], carbohydrates [44, 45], amino acids [46], and proteins. It is understood that the above-mentioned categories are of natural origin and have obvious biocompatibility. Other categories include heterocyclic biomolecules [47], pharmaceutical products, and ionic liquids (Fig. 6) [47]. All of these types of chemicals are abundantly available, environmentally benign, and cost-effective. An additional benefit is that these molecules allow achieving the synthesis of CDs with scalable preparation. Another aspect is that these molecules are composed of chemicals having plenty of heteroatoms (N, S, O, P), which results in the doped form of the CDs, surface passivation, formation of functionalized CDs and no further requirement of post-modification.

5 Luminescence mechanism in CDs

The property of luminescence is an exciting feature of the CDs that has facilitated a myriad of applications of these nanomaterials. For this purpose, endeavor has been made to understand the underlying mechanisms thoroughly. However, the universally acceptable origin of the fluorescence of CDs is still a mystery, and the topic is debatable. CDs are produced by various precursors, employing different techniques, which results in complex components and structures of the resulting CDs. This means that CDs prepared following different synthesis methods, precursor molecules, and post-treatment procedures have varying optical performance, suggesting that the luminescence mechanism of CDs is quite intricate and it is difficult to formulate a unified theory [10]. At present, the most acceptable mechanisms are (i) surface state, (ii) quantum confinement, and (iii) molecular fluorescence.

The surface state effect is the most acceptable luminescence mechanism and includes the degree of surface oxidation and surface functional groups. The oxygen content on the surface of the CDs has a profound influence on the red-shifted emission of the CDs. The greater the degree of surface oxidation, the greater is the number of surface defects [50]. These defects can trap excitons, and the radiation from the recombination of trapped excitons causes the red-shift emission. A series of purified CDs with excitation-independent fluorescence from blue to red is shown in Fig. 7a. The extent of CDs surface oxidation gradually increased along with the red shift of fluorescence emission. In addition, the surface states are also correlated with the surface functional groups, also known as the molecular states, such as C=O and C=N that have proved to be related to CD's fluorescence. Various surface functional groups can cause a diversity of the fluorophores or energy levels in the CDs. The quantum confinement effect is noticed when the size of a particle is too small to be comparable to the wavelength of the electron. The crystal boundary significantly influences the electron distribution when a semiconductor crystal is in the nanometer scale size, which displays some properties such as band-gap and size-dependent energy relaxation dynamics [51]. With an increase in the particle size of the CDs, the absorption peak energy decreases due to the quantum confinement effect (Fig. 7b). It has also been observed that the formation of fluorescent impurities during the bottom-up chemical synthesis (i.e., molecular fluorescence) contributes to the emission from CDs [52]. Molecular fluorophores that were attached to the CDs exert a great influence on the optical properties of the CDs.

6 Application of green synthesized CDs

6.1 Light-emitting diodes

Nowadays, CDs-based LEDs (Fig. 8a) have been prepared by two general strategies: (i) CDs as phosphors and (ii) CDs as active emitters. The former is realized by using CDs as phosphors on a GaN-based UV or blue LED chip, which is frequently used to achieve CDs-based multicolor and white LEDs. Employing CDs as an emissive layer in EL LEDs is the most promising application for flat-panel displays. The CD-based active emission layers and some organic conjugate buffer layer materials are processed by solution processing [53]. Hence, the solubility of CDs in solvents is of significant importance in constructing LED devices. Several CDs have been applied in LEDs as discussed herein. Using citric acid as carbon source,

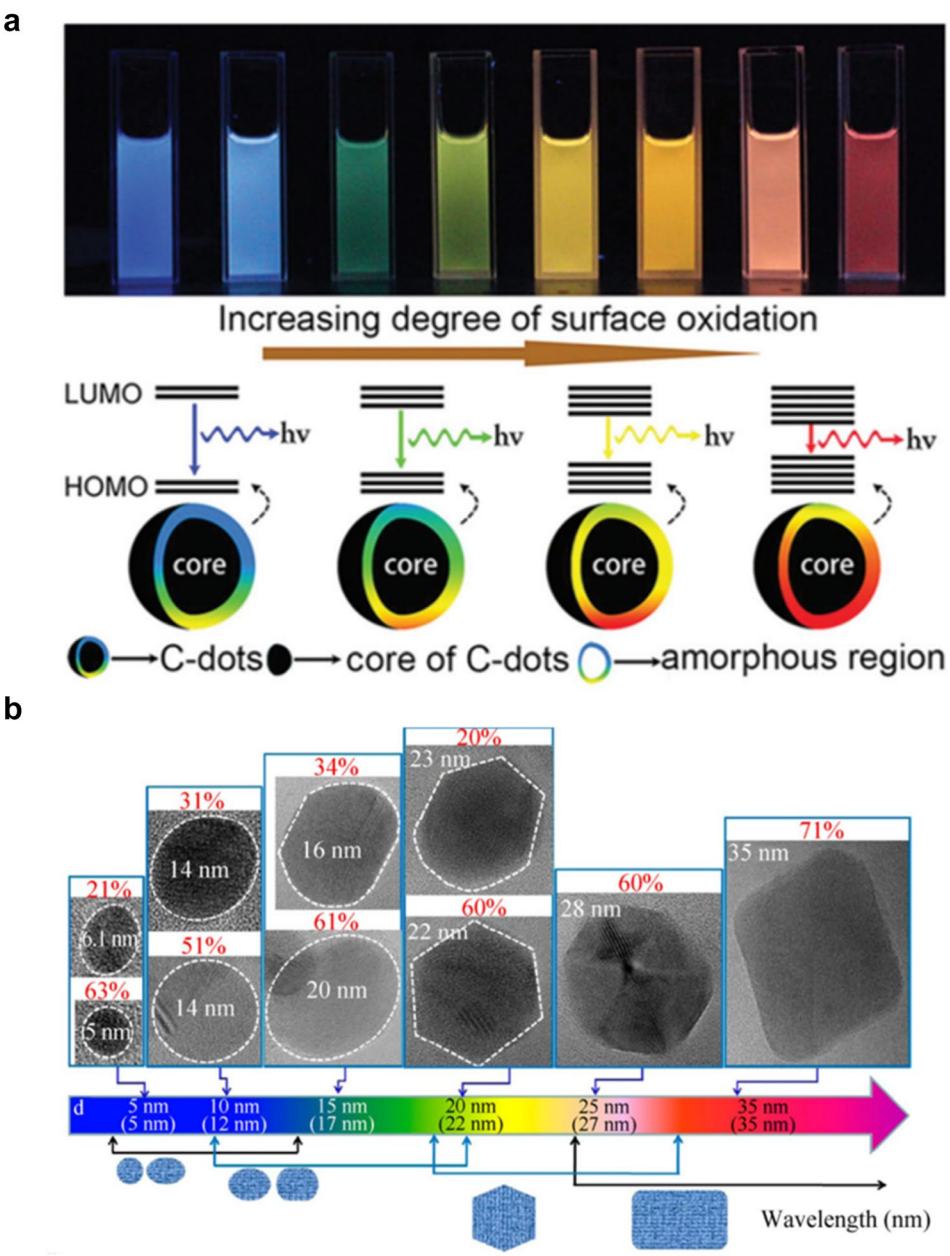

Fig. 7 **a** Mechanism for the fluorescence of CDs based on the degree of surface oxidation [48]; **b** change in fluorescence emission based on variation in the average size of the CDs (shown by the HRTEM images) [49]

1-hexadecylamine-passivated CDs were prepared following pyrolysis [54]. Following the same method, solution-processed inverted white LEDs were prepared [55]. Using banana leaves as the precursor, in a single-step hydrothermal method, CDs were prepared and used as the electron transporting layer (ETL) in organic LED [56]. N-doped CDs were prepared following a single-step hydrothermal treatment using starch as a carbon source and ethylenediamine as N dopant [57]. White LEDs based on starch/CDs composite were prepared, and an ultraviolet LED chip was fabricated. The device emitted white light when operated at 3.0 V. Using ammonium citrate and urea, highly green emissive CDs were prepared following a solid-state reaction method [58]. The CDs depicted green emission with thermal stability from room temperature to 90 °C, and photochemical stability up to 3 h. Following a solvothermal treatment, CDs were prepared using citric acid as a precursor [59]. Bright PL emission from blue to red was observed, following which monochrome LEDs with blue, green, yellow, and red color were prepared. All the LEDs showed stable- and voltage-independent EL emissions. Table 1 provides a list of some CDs prepared using green precursors and their application in LED.

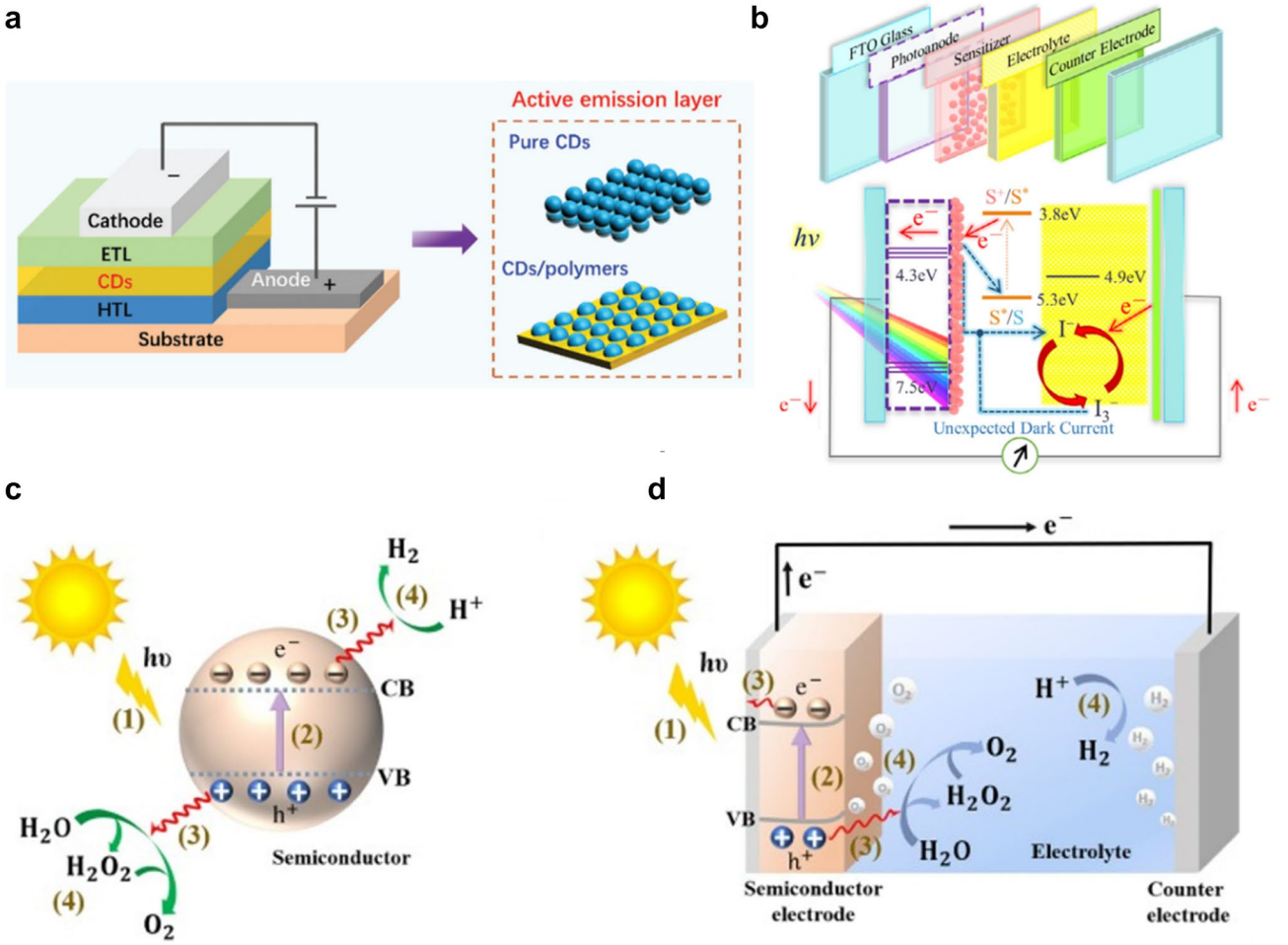

Fig. 8 **a** A typical device structure of CDs-based electroluminescent LED [53]; **b** schematic of the charge transfer process in dye-sensitized solar cells [60]; schematic of **c** photocatalytic and **d** photoelectrochemical hydrogen evolution [61]

Table 1 Structural properties of some green synthesized CDs and their application in LED

Precursor	Preparation condition	Particle size (nm)	Emission properties/emission color	PLQY%	Application	References
Citric acid	Pyrolysis	5	EDPL/–	–	White LED	[54]
Citric acid	Pyrolysis	6 ± 1.9	EDPL/blue	44	White LED	[55]
Banana leaves	Hydrothermal; 125 °C, 7 h	4–6	EDPL/blue	–	OLED	[56]
Starch	Hydrothermal; 200 °C for 16 h	2.22	EDPL/–	9.65	Ultraviolet LED chip	[57]
Ammonium citrate + urea	Solid-state reaction; 200 °C for 1 h	9.3	EDPL/green	13.4	Bioimaging and solid-state LED	[58]
Citric acid	Solvothermal; ethanol 200 °C	1.95 2.41 3.78 4.90 6.68	EIPL/blue Green Yellow Orange Red	75% 73% 58% 53% 12%	Monochrome LEDs with blue, green, yellow, and red color	[59]

6.2 Solar panels

The excellent electrical properties, strong light absorptions, bright photoluminescences, high chemical stabilities, and great electrical conductivities indicate great promise for applications of CDs to a broad range of solar cells. A schematic of the dye-sensitized solar cell (DSSC) is shown in Fig. 8b. Abundant functional groups (e.g., amino, carboxyl, amide, imine, carbonyl) on CD surfaces endow CDs with excellent electron-transfer abilities (i.e., good donor/acceptor characteristics), which enable CDs to be used as electron acceptors [62–64] or donors [65, 66] in solar cells. CDs have been used in different functional layers of solar cells, electron-transporting layers, active absorbing layers, hole-transporting layers, and as interlayer spacing employed to align and adjust the energy levels of other components. Three different CDs were prepared using chitin, chitosan, and glucose and employed for the preparation of solid-state nanostructured solar cells [67]. Layer-by-layer coating of two different types of CDs resulted in the highest efficiency. N-doped CDs were prepared using citric acid and ammonia, following a pyrolysis procedure for 200 °C for 3 h [68]. The N-doping was readily modified by the mass ratio of the reactants. The CDs were green emissive with power-conversion efficiency of 0.79%. Using citric acid and ethanediamine, CDs were in situ grown on TiO_2 surface using the hydrothermal method [69]. A low-cost, environment-friendly CDs-sensitized solar cell was developed with a power conversion efficiency of 0.87%. N-doped CDs were prepared from hydrothermal treatment using strawberry powder as a precursor [70]. The CDs were co-sensitized using commercially available N719 dye to develop a high-performance solar cell with a power conversion efficiency of 9.29%. Using glucose as the precursor, CDs were prepared in a hydrothermal treatment followed by surface modification with PEG [71]. A solar cell prototype was developed co-sensitized with N719 dye and PEG-modified CDs. Table 2 provides a list of CDs prepared using green precursors and their application in solar cells.

6.3 Electrocatalysis

CDs possess excellent electrical transfer/transport capabilities and numerous surface/edge-active sites [62, 72, 73]. Therefore, combinations of CDs with various active metals and semiconductors were used to improve the hydrogen evolution reaction (HER) in electrocatalytic water splitting, and the incorporated CDs provided more interfacial reaction sites. CDs show more abundant heteroatom-doped surface chemistry than other carbon-based nanomaterials such as graphene, CNTs, and diamonds. Figure 8c, d shows the schematic of photocatalytic and photoelectrochemical water splitting. Abundant surface/edge sites and easily modifiable structures of individual CDs make them promising for application to efficient oxygen evolution reaction (OER) processes [74–76]. Further, individual CDs have shown great oxygen reduction reaction (ORR) activities in fuel cells. In addition, CDs are expected to be an important component of electrocatalytic carbon dioxide reduction reaction (CO_2RR) [75, 77–79] and in other electrocatalytic reactions, including alcohol oxidation reactions (AOR) and nitrogen reduction reactions (NRR).

Several research reports are available mentioning the application of CDs in electrocatalysis. An anionic metal organic framework (MOF) was prepared, and following a high-temperature treatment, CDs were obtained [80]. The synthesized CDs showed electrocatalytic activity as a metal-free catalyst for the oxygen reduction reaction (ORR). The incorporation of Co nanoparticles improved the catalytic activity and stability. In a one-pot hydrothermal synthesis using citric acid and dicyandiamide, N, S-doped CDs were obtained [81]. The N, S-doped CDs showed efficient oxygen electrocatalytic activity comparable to noble metals. In another study, CDs were prepared following a hydrothermal

Table 2 Structural properties of some green synthesized CDs and their application in solar cells

Precursor	Preparation condition	Particle size (nm)	Emission properties/emission color	PLQY%	Application	References
Chitin Chitosan Glucose	–	14.1 ± 2.4 8.1 ± 0.3 2.57 ± 0.04	EDPL/blue	–	Solid-state nanostructured solar cells	[67]
Citric acid + ammonia	Pyrolysis; 200 °C, 3 h	10.8	EDPL/blue	36	Solar cells	[68]
Citric acid + ethanediamine	Pyrolysis; 180 °C, 24 h	2–6	–	–	CDs-sensitized solar cells	[69]
Strawberry powder	Hydrothermal; 170 °C, 3 h	3.01	EDPL/blue	–	N_{300}-CQDs/N719 co-sensitized DSSC	[70]
Glucose	Hydrothermal; 195 ± 5 °C, 6 min	2–3	EDPL/blue	–	PEG-*m*-CQDs/N719 co-sensitized DSSC	[71]

Table 3 Structural properties of some green synthesized CDs and their application in electrocatalysis

Precursor	Preparation condition	Particle size (nm)	Emission properties/emission color	PLQY%	Application	Reference
Anionic MOF {[Mg_3(ndc)$_2$·5(HCO_2)$_2$(H_2O)]·[NH_2Me_2]·2H_2O·DMF}	Pyrolysis; 500 °C, 6 h	< 10	EDPL/blue	–	Electrocatalytic ORR activity	[80]
Citric acid + dicyandiamide	Hydrothermal; 180 °C, 6 h	8.5	–	–	Electrocatalyst for both OER and ORR	[81]
Citric acid + urea	Hydrothermal; 180 °C, 12 h	5–7	–	–	ORR activity	[82]
Citric acid + ethylenediamine	Hydrothermal; 200 °C, 8 h	20–80 (size of composite)	–	–	Electrocatalyst for both OER and ORR	[83]
Glucose + dicyandiamine	Hydrothermal; 200 °C, 6 h	3.4	EDPL/blue	–	OER activity	[84]
Willow leaves	Hydrothermal; 180 °C, 24 h	2–4	EDPL/blue	–	Electrocatalytic ORR activity	[85]

treatment of citric acid and urea, followed by N-doping using pyrrole [82]. The obtained N-CDs were successfully applied as synergistic agents with tungsten nitride for electrocatalysis of ORR. CDs were hydrothermally synthesized using citric acid and ethylenediamine, and a composite with Co_9S_8 nanoparticles was prepared [83]. In the presence of this system, aniline was polymerized to afford effective catalysts for both OER and ORR in high-performance Zn–air batteries. CDs were prepared from glucose and dicyandiamine following a one-pot hydrothermal synthesis route [84]. A nitrogen-doped carbon-encapsulated cobalt nanoparticles (N–C@Co NPs) system was in situ constructed that acted as an efficient electrocatalyst for OER in water splitting. Following hydrothermal treatment of willow leaves, N-doped CDs were prepared and utilized for ORR [85]. The activity was comparable to commercially available Pt/C catalyst. Table 3 provides a list of some CDs prepared using green precursors and their application in electrocatalysis.

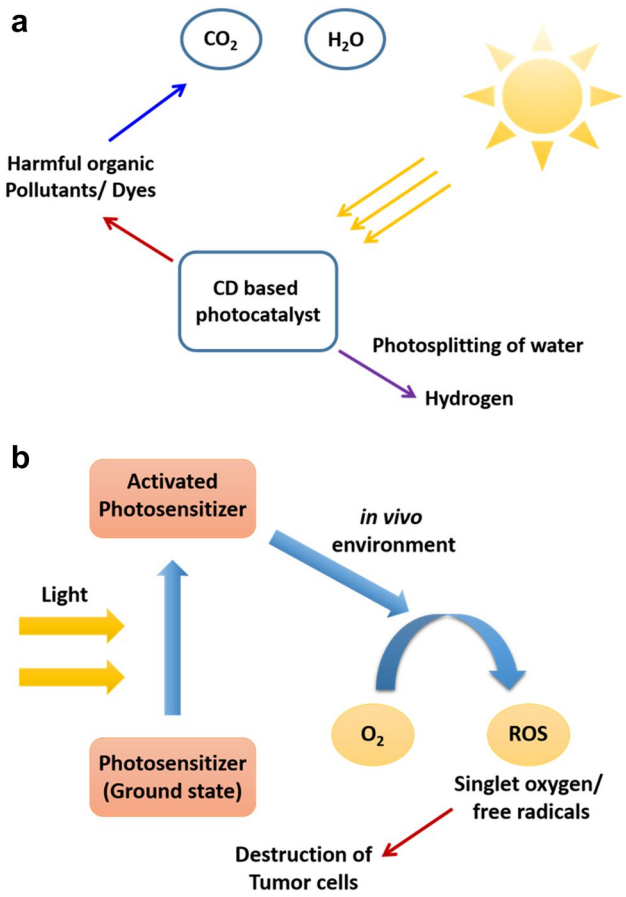

Fig. 9 Principles of **a** photocatalysis by CDs; and **b** photodynamic therapy for cancer treatment

6.4 Photocatalysis

Nanomaterials have found extensive application in photocatalysis in recent years [86, 87]. CDs have also been utilized as effective catalysts for the degradation of a number of organic dyes and in photo-splitting of water for hydrogen production [88, 89] (Fig. 9a). Ashes of the eggshell membrane were subjected to MW irradiation for 1 min to produce CDs having a size < 10 nm [90]. The synthesized CDs were highly fluorescent under UV irradiation. Under sunlight irradiation, the CDs successfully degraded methylene blue dye in the range of 26–43% at 5–1 mg L^{-1} of the dye. CDs were prepared via US treatment and further subjected to sol–gel treatment and spin coating to obtain a heterostructure of ZnO/CDs [91]. The material was successfully applied in the photocatalytic degradation of Rhodamine B. Following ultrasonication in molten Ga and PEG-400

Table 4 Structural properties of some green synthesized CDs and their application in photocatalysis

Precursor	Preparation condition	Particle size (nm)	Emission properties/emission color	PLQY%	Application	References
Eggshell membrane	560 W, 2 min	3.88 ± 0.56	SDPL/blue	5	Degradation of methylene blue	[90]
Graphite powder, H_2SO_4 and HNO_3	2 h	3	SDPL/green, yellow	–	Photocatalysis	[91]
Molten Ga, PEG-400	120 min, 50% amplitude	5 ± 2	EDPL/violet blue	2	Production of ROS for biomedical application	[92]
Waste polyethylene terephthalate plastic bottles	Pyrolysis 120 °C, 6 h	3	–	–	Separable production of 5-hydroxymethylfurfural at low temperature	[93]
D-Glucose, ionic liquid	MW	12 ± 2	–	–	Production of H_2O_2	[94]

as the precursor, Ga-doped CDs (Ga@CDs) were prepared [92]. A greater photosensitization was shown in doped CDs compared to the pristine CDs. Waste polyethylene terephthalate bottles were used as a precursor via air oxidation and sulfuric acid-assisted hydrothermal treatment [93]. The synthesized CDs were used in catalytic dehydration of fructose to 5-hydroxymethylfurfural (HMF) at low temperatures, leading to high yields (up to 97.4%) of HMF. MW synthesis of N-doped CDs was performed in the presence of D-glucose and 1-ethyl-3-methylimidazolium ethylsulfate in aqueous medium [94]. The synthesized CDs were used as a metal-free catalyst for the selection and production of H_2O_2. Table 4 provides a list of some CDs prepared using green precursors and their application in photocatalysis.

6.5 Photodynamic therapy

Photodynamic therapy is an advanced biomedical technique wherein energy transfer can be applied for the destruction of damaged cells and tissues [95–97]. This method is helpful in cancer treatment because it efficiently targets the malignant tissue leading to its destruction without harming normal healthy tissue [98]. The photodynamic therapy procedure employs a photosensitizer (a photosensitive molecule that can be localized in the target biological environment) and an activator (which activates the photosensitizer by transmitting a suitable wavelength light), both of which should be non-cytotoxic [95, 99]. Reactive oxygen species [ROS, e.g., superoxide ($O_2^{\cdot-}$), hydroxyl radical ($^{\cdot}OH$), and/or singlet oxygen ($^1O_2$)] are generated by the photosensitizer via the transfer of energy from photons to molecular oxygen. These ROS species cause cytotoxic effects, and their action is specific to

Table 5 Structural properties of some green synthesized CDs and their application in photodynamic therapy

Precursor	Preparation condition	Particle size (nm)	Emission properties/emission color	PLQY%	Application	References
Cannabis sativa leaf extract	Room temperature stirring for 1 h	5	–	13%	Bactericidal activity against *Escherichia coli* and *Staphylococcus aureus*	[104]
Metronidazole	Hydrothermal 250 °C for 3 h	2.9	EDPL/multicolor	28.1	Antibacterial activity against *Porphyromonas gingivalis*	[105]
Wheat bran	Hydrothermal 180 °C for 3 h	2.5–8.5	EDPL/blue-green	33.23	Drug delivery agent for Amoxicillin for antibacterial activity against *S. aureus,* and *E. coli*	[106]
Arginine, lysine, histidine, cysteine, methionine	MW	5–20	EDPL/blue	10–38	Antibacterial activity against *S. aureus,* and *E. coli*	[107]
Citric acid	MW	3.81	–	–	In vivo antibacterial activity against *S. aureus*	[16]

the target cells/tissues exposed to light [95]. This photo-induced toxicity can kill malignant tumors or cancer cells [98] (Fig. 9b). For the purpose of antimicrobial activity, it is a combination of a non-toxic photosensitizer and light of a suitable wavelength that can interact with molecular oxygen to afford ROS that can selectively kill pathogenic microbial cells [23, 96]. Several reports are available in the literature on the antimicrobial activity of CDs synthesized via different procedures [100, 101]. The CDs are tested as antimicrobial agents in vitro and in vivo against Gram-positive and Gram-negative bacteria. Furthermore, CDs–drug conjugates and metal-doped CDs are reported to show enhancement in antimicrobial action. Table 5 provides a list of CDs prepared using green precursors and their application in photodynamic therapy.

Folic acid (FA)-functionalized CDs were developed as carriers for the PS zinc phthalocyanine (ZnPc) for simultaneous bioimaging and targeted photodynamic therapy in cancer cells [102]. CDs were surface passivated using PEG and loaded with the photosensitizer zinc phthalocyanine (ZnPc). CD-PEG-FA/ZnPc exhibited excellent imaging and therapy of cancer cells. N- and S-doped CDs were prepared using citric acid and thiourea following hydrothermal treatment and used for photothermal therapy (PTT) in mouse models [103]. Using *Cannabis sativa* leaf extract, CDs and Ag@ CDs were prepared [104]. The structural characterization revealed functional groups from the aromatic, carboxylated, and hydroxylated moieties. The synthesized CDs showed remarkable antibacterial behavior against *E. coli* and *S. aureus*. Highly photoluminescent CDs were prepared from metronidazole, a widely used antibacterial drug, following a hydrothermal approach [105]. The synthesized CDs were successfully utilized in the growth inhibition of *Porphyromonas gingivalis*. Using wheat bran as green precursor, CDs were prepared having high QY of 33.23% [106]. The synthesized CDs were used for the preparation of conjugate with drug amoxicillin (AMX), and the CD–AMX conjugate was used for antibacterial activity against Gram-positive and Gram-negative bacteria. N- and S-doped CDs were produced via MW irradiation from amino acids arginine, lysine, histidine, cysteine, and methionine [107]. The synthesized CDs showed a minimum inhibitory concentration (MBC) of 1 mg L^{-1} against Gram-positive and Gram-negative bacteria. One-pot MW synthesis of CDs was carried out using citric acid as precursor and investigated in vitro and in vivo (in mice) against *S. aureus* bacteria [16]. Complete healing of the wounded tissue in mice was observed.

6.6 Bioimaging

Imaging of cells and tissues is an important aspect relevant to the diagnosis of various diseases, especially cancer.

Table 6 Structural properties of some green synthesized CDs and their application in bioimaging

Precursor	Preparation condition	Particle size (nm)	Emission properties/emission color	PLQY%	Application	References
Crab shells	–	8	EDPL/blue	14.5	Imaging cancer cells	[39]
Gelatin hydrolysate	30 min	3.8	EDPL/blue	33.8	Bioimaging and anti-counterfeiting	[37]
Citric acid + triethylenetetramine (TETA)	Thermal pyrolysis	3.07 ± 0.43	EDPL/green	11.4	In vivo bio-imaging of HepG2 cells	[114]
tetraethylenepentamine (TEPA)		3.16 ± 0.53		10.6		
polyene polyamine (PEPA)		3.73 ± 0.33		9.8		
Andrographis paniculata (Kalmegh)	Hydrothermal 160 °C for 8 h	9	EDPL/blue	15.10	Imaging of human breast carcinoma cells (MCF-7)	[115]
Bovine gelatin	Hydrothermal 200 °C for 3 h	59	EDPL/blue	–	Anticancer and bioimaging applications	[116]
PHM3 microalgae strain	200 °C for 3 h	67	EDPL/green			
Glycerol, glycol, glucose, sucrose	MW	1.1 ± 0.42 2.1 ± 0.76	EDPL/blue, green	5.8	Biolabeling and Bioimaging	[34]
Milk	MW	3	EDPL/blue	–	Imaging of HeLa cells	[117]
Sucrose	MW	5	EDPL/green	2.4	Imaging of C6 glioma cells	[118]
Glutathione	MW	–	–	16.8	Deep-tissue two-photon bioimaging and drug delivery	[119]

Several systems having considerable fluorescence have been reported for bioimaging purposes. These include organic and inorganic dyes and nanoparticles [108–110]. The incorporation of carbon nanomaterials in this application presents a primary advantage in the lack of metal ions that can adversely influence the in vivo environment via cytotoxicity. The suitable agent for bioimaging should possess biocompatibility, tunable emission spectra, and lack of cytotoxicity. The advent of nanomaterials has found application not only in bioimaging for diagnosis, but also in therapy. The theranostic applications are performed by functionalizing the molecules of the required chemical to the fluorescent nanomaterial via chemical functionalization. A number of quantum dots such as ZnO, GQDs, and CDs have been reported for the imaging application of living cells [111, 112]. The CDs produce attractive optical features, viz., up-conversion photoluminescence, piezo-chromic fluorescence, solid-state fluorescence, excitation-dependent emission, and phosphorescence. Due to their excellent photoluminescence behavior, CDs are reported as a potential agent for bioimaging of cells in both in vitro and in vivo conditions (Fig. 11a). Cao et al. first reported the application of CDs in bioimaging in vitro and in vivo [113]. Table 6 provides a list of some CDs prepared using green precursors and their application in bioimaging.

A sonochemical approach was adopted to produce N-doped CDs from crab shells showing excellent water solubility and high quantum yield [39]. The synthesized CDs were applied as nanoprobes to target imaging of cancer cells. Gelatin hydrolysate was used as a green precursor via the US method within 30 min [37]. The developed CDs were employed in the application of cell imaging and anti-counterfeiting. Using citric acid, triethylenetetramine (TETA), tetraethylenepentamine (TEPA), polyene polyamine (PEPA), CDs having sizes of the order of 3 nm and green color PL emission with QY of 9–11% [114] were produced. Figure 10 shows the synthesized CDs samples' TEM, HRTEM, and XPS survey scan spectra. The TEM images indicate uniform particle size distribution without any aggregation, with the lattice planes showing spacing of 0.21 nm and 0.245 nm corresponding to (103) diffraction plane of diamond-like (sp^3) carbon and (100) facet of graphitic carbon, respectively. The XPS spectra show considerable N-doping with an increase in the N content of the passivating agents. The synthesized CDs were employed for the in vivo bioimaging of HepG2 cells. *Andrographis paniculata* (Kalmegh), an Ayurvedic medicinal plant, was used as a precursor for the production of CDs [115]. The synthesized CDs were successfully utilized in cellular imaging of human breast carcinoma cells. In addition to the natural products, carbohydrates, and amino acids, CDs have also been synthesized using protein molecules as discussed above. In another study, CDs were prepared from gelatin protein and from algal biomass of *Pectinodesmus* sp. via the hydrothermal method [116].

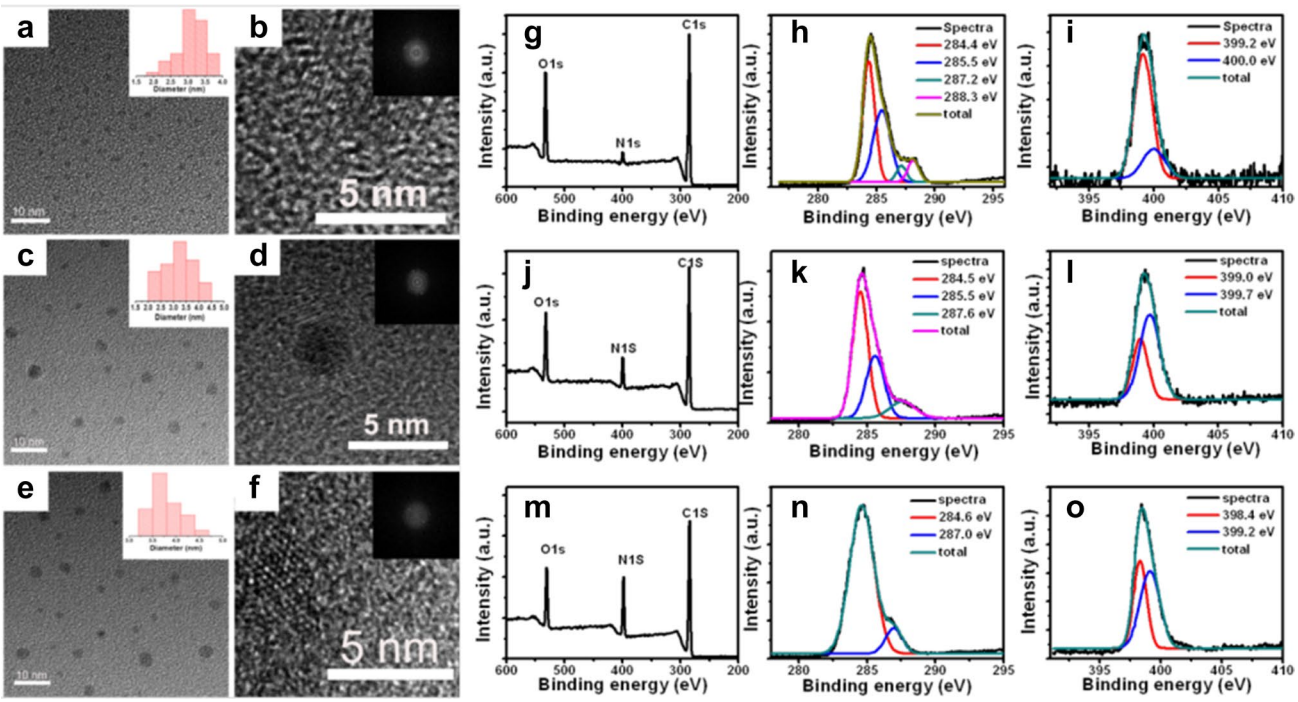

Fig. 10 TEM (**a**–**e**) and HRTEM (**b**–**f**) of CDs-TETA (**a**, **b**), CDs-TEPA (**c**, **d**) and CDs-PEPA (**e**, **f**). Inset: corresponding particle size distributions and fast Fourier transform images. XPS (**g**, **j**, **m**), XPS C1s (**h**, **k**, **n**), and XPS N1s (**i**, **l**, **o**) spectra of CDs-TETA, CDs-TEPA and CDs-PEPA, respectively [114]

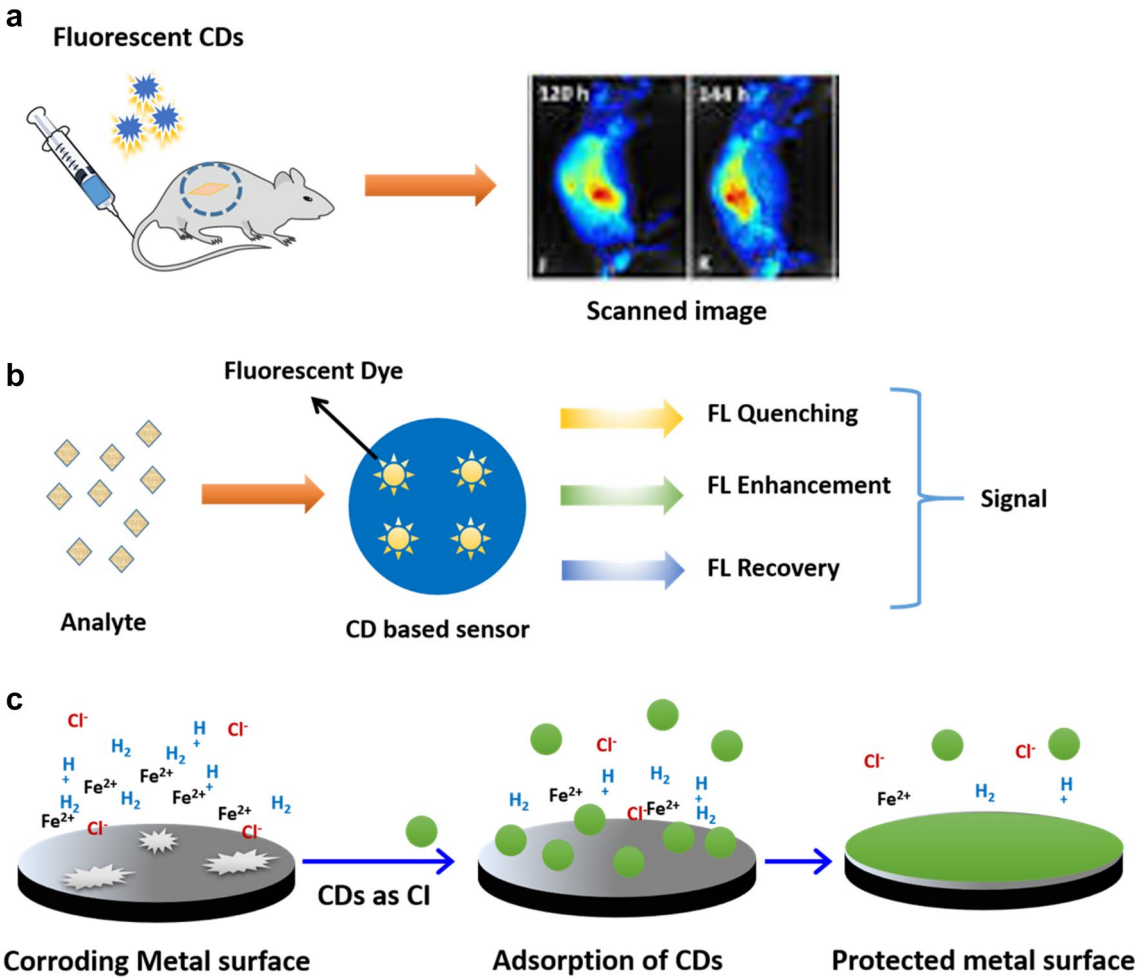

Fig. 11 Principles of **a** bioimaging using CDs; **b** CDs-based sensors; and **c** CDs as corrosion inhibitors

The gelatin-synthesized CDs displayed activity in the imaging of plant and bacterial cells. On the other hand, the CDs from the algal source had anticancer applications. CDs were prepared following a single-step MW irradiation of carbohydrates without employing any surface passivating agents [34]. The synthesized CDs were biocompatible and cell permeable and were applied successfully in bio-labeling and bioimaging. Fluorescent N-doped CDs were prepared from milk that were well-dispersed in an aqueous medium [117]. The synthesized CDs were employed in the bioimaging of HeLa cells. Using sucrose as precursor and diethylene glycol as the reaction medium, CDs were prepared following the MW irradiation method [118]. The CDs were well dispersed in an aqueous medium with a bright green luminescence. The application was reported for the bioimaging of C6 glioma cells. Following MW heating of glutathione, near-infrared emissive CDs were prepared and utilized for deep tissue bioimaging and drug delivery [119].

6.7 Chemical sensors

There is a growing research interest in the application of nanomaterials as chemical/biosensors [120–122]. A number of reports are available on the application of metal nanoparticles, carbon nanomaterials, and semiconductor nanostructures for sensor development. CDs have been extensively reported for sensor development [111, 122–124]. Employing the fluorescence activity and surface functionalization of CDs, several sensors for chemical and biological species have been developed using CDs. The CDs have interesting features such as bright and intense fluorescence emission in the visible range, fluorescence quenching by the target analyte, variable emission spectra, negligible cytotoxicity, and feasibility of preparation. The general working principle of the CDs-based sensor is shown in Fig. 11b. Table 7 provides a list of some CDs prepared using green precursors and their application in sensor development.

Using citric acid, amino acid L-cysteine, and the polysaccharide dextrin, in a one-step MW method, highly fluorescent

Table 7 Structural properties of some green synthesized CDs and their application in sensors

Precursor	Preparation condition	Particle size (nm)	Emission properties/emission color	PLQY%	Application	References
Citric acid, L-cysteine, dextrin	800 W, 3 min	2.61	SDPL/blue	22	Detection of copper ions	[125]
Lactose, HCl	600 W, 15 min	–	EIPL/blue	–	Analysis of heterocyclic aromatic amines	[126]
Glucose, H_3PO_4	700 W, 5 min	4.5–13.5	EIPL/yellow	8	Cr(VI) sensing	[127]
BSA, urea	700 W, 5 min	2.4–5	EDPL/blue, green	14	pH and temperature sensing	[128]
Xylose	200 °C, 10 min	8.43 nm	EDPL/green-yellow	42.44	pH sensing	[129]
Xylose	220 °C, 200 °C, 180 °C, 10 min	6.80	EDPL/green	73.6	Anti-counterfeit printing	[33]
		7.23	EDPL/green	56.1		
		6.80	EDPL/green	40.9		
		9.88	EDPL/green	65.3		
		8.83	EDPL/green	49.5		
		6.87	EDPL/green	42.8		
		16.37	EDPL/blue	8.0		
		10.70	EDPL/blue	6.8		
Lemon extract	150 W, 1 h	60	EDPL/green	–	Identification of toxic metal ions and bacteria *Pseudomonas aeruginosa*	[130]
D-Fructose	60 s, 10% amplitude	2.5	EDPL/	–	Methylmercury detection	[38]
Citric acid + thiourea	Hydrothermal 160 °C, 8 h	3.2	EDPL/faint yellow EDPL/bright blue	–	Fluorescent detection of living cancer cells (HepG2)	[131]
Tryptophan	Hydrothermal, 180 °C, 12 h	3.0 ± 0.4 to 6.0 ± 0.4	EDPL/blue	55.6	Array-based protein sensing	[132]
Arginine				48.6		
Cysteine				45.6		
Phenylalanine				62.1		
Glutamine				39.0		
Leucine				50.4		
Histidine				61.8		
Tyrosine				51.5		
Glycine				38.4		
Cysteine	Hydrothermal, 160 °C, 3 h	6	EDPL/	18 ± 4	Sensing of metal cations	[133]
Histidine		6		25 ± 4		
Lysine		5		19 ± 2		
Arginine		6		27 ± 4		
Grape skin	Hydrothermal	4.0 ± 1.5	EDPL/green	18.67	Picric acid detection	[5]
Gardenia flowers	Hydrothermal 180 °C for 6 h	9	EDPL/blue	9.82	Detection of metronidazole in pharmaceuticals and rabbit plasma	[134]
Azadirachta indica	Hydrothermal 150 °C for 4 h	3.2	EDPL/blue	27.2	Detection of H_2O_2 and ascorbic acid in common fresh fruits	[135]
Citric acid + thiosemicarbazide	Hydrothermal 180 °C for 5 h	1.2 to 2.4	EDPL/blue	37.8	Detection of picric acid in aqueous solution and living cells	[136]
Dunaliella salina biomass	Hydrothermal 200 °C for 3 h	4.7	EDPL/blue	8	On–off sensing of Hg(II), Cr(VI) and live cell imaging	[137]

Table 7 (continued)

Precursor	Preparation condition	Particle size (nm)	Emission properties/emission color	PLQY%	Application	References
Histidine + thiourea	Hydrothermal 220 °C for 3 h	2.9	EDPL/blue	46	Colorimetric detection of H_2O_2 and glutathione in human blood serum	[138]
Jatropha fruits	Hydrothermal 180 °C for 5 h	3.2	EDPL/bright blue	13.7	Fluorometric sensor for the detection of chlorpyrifos pesticide	[139]
Latex of *Euphorbia milii*	Hydrothermal 180 °C for 3 h	3.4 ± 0.45	EDPL/blue	39.2	Detection of glutathione in human blood serum	[140]
Mustard seeds	Hydrothermal 180 °C for 4 h	4.58 ± 0.26	EDPL/blue	–	Colorimetric detection of H_2O_2 and ascorbic acid in a real sample	[141]

CDs having a size of 2.61 nm were obtained [125]. The CDs were N, and S doped and showed efficient performance in Cu^{2+} ion detection. Using lactose as precursor and the MW method, CDs were prepared and applied as a nanosensor platform for the detection of heterocyclic amines in the range of concentration 0.35–0.45 mg L^{-1} [126]. Amphibious

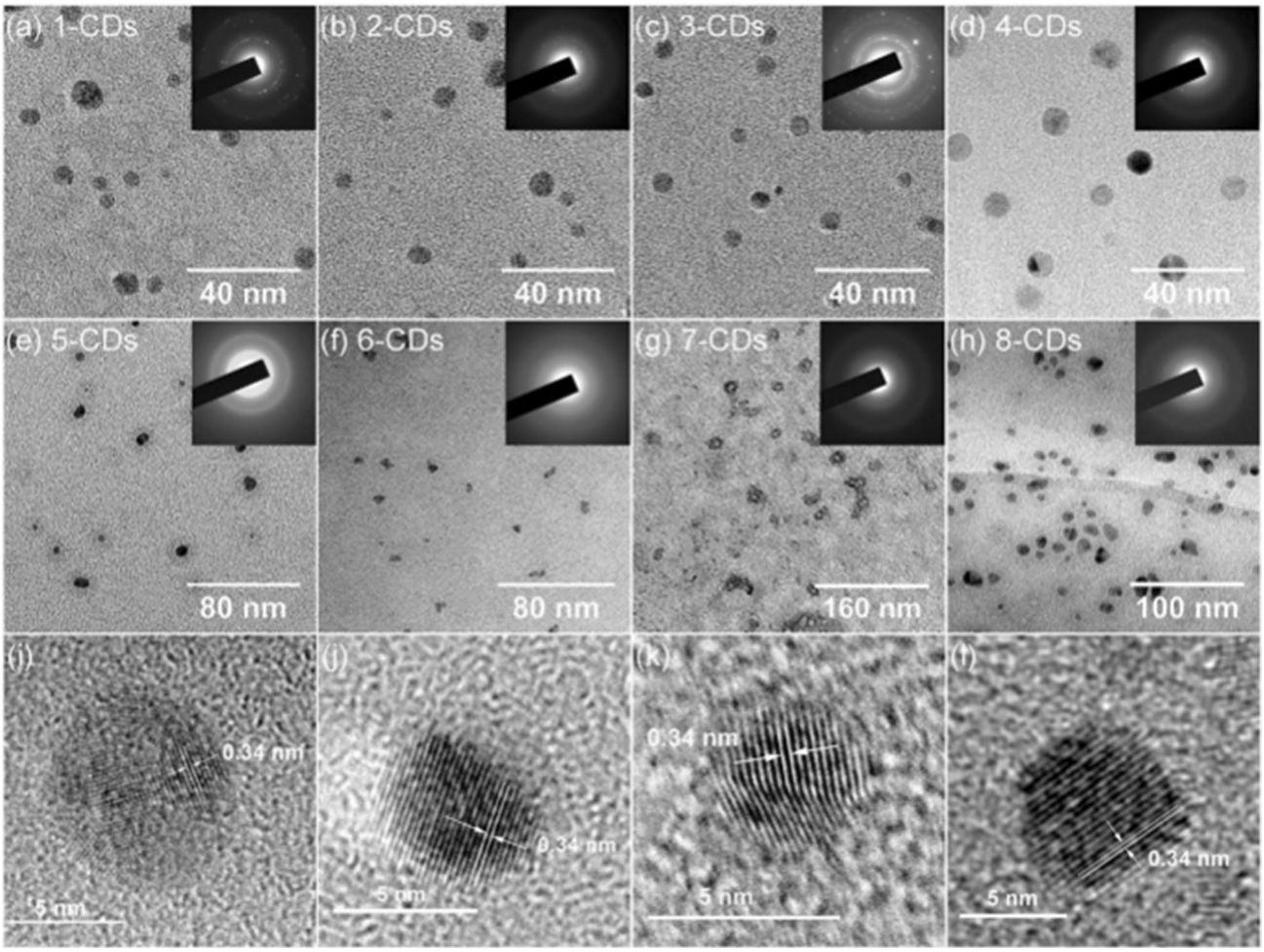

Fig. 12 **a–h** TEM images of different CDs samples from 1-CDs to 8-CDs, with insets showing corresponding SAED patterns; **i–l** HRTEM of 1-CD, 2-CDs, 3-CDs and 4-CDs [33]

yellow emitting CDs were prepared using a rapid MW method and applied as a colorimetric nanosensor for the discrimination of Cr(III) and Cr(VI) [127]. Using bovine serum albumin (BSA) and urea as the precursor, highly photoluminescent CDs were synthesized in one-step MW treatment [128]. A multifunctional fluorescent nanosensor for pH and temperature was developed using the CDs. This method suggested the development of CDs using other protein-based sources, e.g., lipase and trypsin, and application in metal ion detection. In other studies, xylose-derived CDs having N, and S doping were developed via MW treatment and application in anti-counterfeiting [129] and pH sensing was explored [33]. Figure 12 shows the diffraction patterns and rings of CDs samples synthesized using xylose as precursor employing MW at different conditions [33]. The HRTEM images display a clear lattice spacing of 0.34 nm consistent with the (002) lattice plane of graphite. Lemon extract was used as a green and biocompatible precursor to develop CDs following the US method [130]. The synthesized CDs were used to prepare $MgFe_2O_4$-CDs nanocomposite, which was utilized in the fluorescence detection of Ni (II), Cd (II), Hg (II) ions and *Pseudomonas aeruginosa*. D-fructose was used as a green precursor for the sonochemical synthesis of CDs having average size of 2.5 nm and a narrow size distribution [38]. The synthesized CDs were utilized for preparation of a fluorescent nanoassay for detection of methylmercury.

Using citric acid and thiourea, in a hydrothermal treatment, CDs were prepared having faint yellow to bright blue emission colors [131]. The synthesized CDs were used as a selective and cost-effective nanoprobe for the detection of living cancer cells. Citric acid was subjected to hydrothermal treatment in the presence of a series of amino acids to develop amino acid-functionalized CDs [132]. High QY up to 62% was achieved with tunability of surface charge and hydrophobicity. The synthesized CDs were used in array-based protein sensing. In another study, CDs were modified using ethylenediamine and different amino acids and studied for sensing metal cations via the fluorescence quenching method [133]. The decrease in the fluorescence intensity was found to be in direct proportion with the increasing concentration of metallic ions. CDs were prepared via the hydrothermal method employing grape skin as precursor [5]. The synthesized CDs were employed for the picric acid detection via fluorescence quenching in real water samples. Fluorescent CDs were prepared from gardenia plant following a hydrothermal synthesis procedure [134]. The synthesized CDs were applied in the sensing of metronidazole based on fluorescence quenching in pharmaceuticals and rabbit plasma.

Fluorescent CDs were prepared from leaf extract of *Azadirachta indica* and used for peroxidase-mimetic activity for detection of H_2O_2 and ascorbic acid in fresh fruit samples [135]. The peroxidase-mimetic activity was studied toward the oxidation of peroxidase substrate 3,3′,5,5′-tetramethylbenzidine (TMB) with H_2O_2. Using citric acid and thiosemicarbazide, N, S-co-doped CDs were prepared using the hydrothermal method [136]. The synthesized CDs were used for selective detection of picric acid in an aqueous solution and in living cells. Using algal biomass of *Dunaliella salina*, N, P-doped CDs were prepared following the hydrothermal method [137]. The CDs exhibited blue color under UV light with a QY of 8%. The CDs were used for intracellular detection of Hg (II) and Cr (VI). N, S-doped CDs were prepared from histidine and thiourea with an excellent QY of 46% [138]. The synthesized CDs showed efficient performance for the detection of H_2O_2 and glutathione in human blood serum samples. CDs were prepared from *Jatropha* fruit following hydrothermal method of synthesis with a high QY of 13.7% [139]. The CDs were applied for the detection of pesticides in environmental and agricultural samples with a limit of detection 2 ng L^{-1}. The latex of *Euphorbia milii* was successfully employed in the development of CDs via hydrothermal treatment [140]. The synthesized CDs were applied for the detection of glutathione in human blood serum. Mustard seeds were used to prepare CDs via hydrothermal technique and employed for a peroxidase-like mimetic activity for colorimetric detection of H_2O_2 and ascorbic acid in real samples [141].

6.8 Corrosion protection

Corrosion can be described as the natural degradation of metallic materials upon exposure to the environment to the ore forms from where the original metallic form was extracted and purified [21, 142, 143]. This process can be aggravated by the presence of extreme environments, e.g., seawater, alkaline conditions, acidic media, high temperatures, and flow conditions. Severe damage to the metallic structures takes place under such conditions. This results in a considerable detrimental effect to the surfaces of metals and can lead to the potential failure of structures, environmental pollution, economic losses, and even hazards to human life. Different forms of corrosion include pitting, uniform corrosion, crevice formation, galvanic corrosion, stress corrosion, intergranular corrosion, and erosion corrosion [144, 145]. The global loss of corrosion amounts to about USD $2.4 trillion, which is around 3.4% of the global GDP [146]. To address this issue, one of the commonly used methods is the application of corrosion inhibitors. A corrosion inhibitor, by definition, is a chemical additive, which, when added to a corrosive medium, retards the rate of corrosion. Generally, inorganic inhibitors such as nitrates, nitrites, chromates, and phosphonates are applied in the industries. The organic inhibitors commercially used include imidazolines, amides, acetylenic alcohols, etc. These categories are highly toxic and carcinogenic, and hence their usage is discouraged

by the environmental regulatory bodies across the globe. Environmentally benign and green molecules are being put forward as corrosion inhibitors, such as heterocyclic biomolecules, ionic liquids, natural extracts, carbohydrates, amino acids, proteins, and pharmaceutical products. From the above sections, it can be noted that the same molecules also act as novel and environmentally benign precursors for the synthesis of CDs.

Conventionally, the nanomaterials such as metal oxides, graphene, and graphene oxide (GO) find application in the preparation of anti-corrosion coatings. This is owing to their hydrophobic behavior, impermeability, chemical stability, and barrier action [2, 147–149]. Extensive research is available on the application of graphene and GO-based coatings. In addition, other nanomaterials such as ZnO, TiO_2, NiO, montmorillonite [150], and graphydine [151] have also been utilized in the development of coatings. The nanosized

Table 8 Performance comparison of some green CDs-based corrosion inhibitors

Precursor	Method	Metal surface/corrosive medium	C_R/I.E. (%)/inhibitor concentration	References
4-Aminosalicylic acid	Solvothermal 200 °C, 20 h	Copper/0.5 M H_2SO_4	–/89.2/50 mg L^{-1}	[173]
4-Aminosalicylic acid	Solvothermal 200 °C, 18 h	Q235 carbon steel/1 M HCl	–/87.2/100 mg L^{-1}	[174]
4-Aminosalicylic acid	Solvothermal 200 °C, 16 h	Carbon steel/CO_2 saturated 3.5% NaCl	0.08 g cm^{-2} h^{-1}/93.0/50 mg L^{-1}	[175]
4-Aminosalicylic acid and L-histidine	Solvothermal 200 °C, 12 h	Q235 steel/1 M HCl	91.5/50 mg L^{-1}	[176]
Citric acid + L-histidine	Reflux 200 °C, 1 h	Q235 steel/0.1 M HCl	96.13/200 mg L^{-1}	[177]
Citric acid + L-serine	Hydrothermal 200 °C, 18 h	Copper/0.5 M H_2SO_4	98.5/200 mg L^{-1}	[178]
Citric acid + imidazole ionic liquid	Hydrothermal 200 °C, 30 min	Q235 steel/1 M HCl, 3.5% NaCl	92.60/200 mg L^{-1} 83.45/200 mg L^{-1}	[179]
Citric acid + isoniazid + thiourea	Hydrothermal 180 °C, 6 h	Mild steel/15% HCl	98.64/200 mg L^{-1}	[180]
Tryptophan	Pyrolysis 160–200 °C, 0.5–2 h	Q235 carbon steel/1 M HCl	91/200 mg L^{-1}	[181]
Folic acid + o-phenylenediamine	Hydrothermal 200 °C, 6 h	Q235 steel/1 M HCl	95.4/150 mg L^{-1}	[182]
Glucose + ascorbic acid + 4-amino-3-hydrazine-5-mercapto-1,2,4-triazole	Hydrothermal 180 °C, 4 h	Copper/3.5% NaCl	88/70 mg L^{-1}	[183]
Dopamine	Hydrothermal 180 °C, 6 h	Q235 steel/1 M HCl	96.1/400 mg L^{-1}	[184]
Coffea canephora + urea	Pyrolysis 220 °C, 5 h	Copper/1% NaCl	84.94/1 g L^{-1}	[185]
Durian juice	Pyrolysis 125 °C, 12 h	Copper/1% NaCl	86/800 mg L^{-1}	[186]

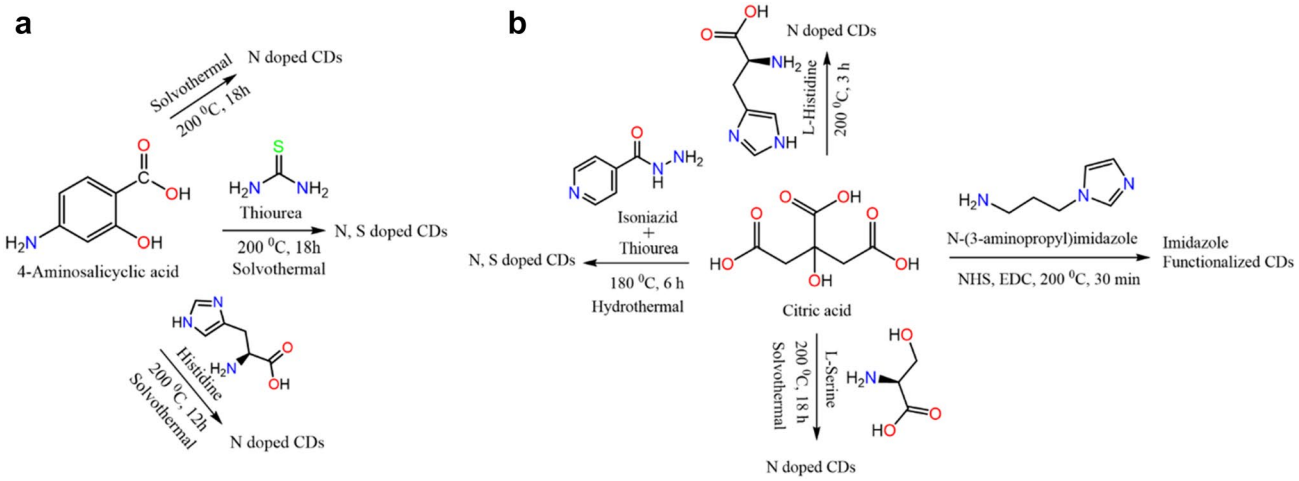

Fig. 13 Schemes for the synthesis of CDs employing hydrothermal and solvothermal methods using **a** 4-aminosalicylic acid [174–176] and **b** citric acid [177–180] in the presence of some amino acids

materials are used to cover the pores in the coatings, enhance the surface coverage of the coating on the underlying metallic substrate, and improve the hydrophobicity of the coatings. Conventionally reported corrosion inhibitors are based on heterocyclic molecules and polymers [24, 29, 152–157]. Considering the importance of nanomaterials, researchers have also explored the polymer composites of AgNp with biopolymers as corrosion inhibitors [158–160] and polymer–ZnO nanocomposites [161].

In the past few years, several reports have come in the literature focusing on the application of functionalized GO-based corrosion inhibitors [162–172]. The oxygen-containing polar functional groups, e.g., –C=O, –OH, –COOH, etc., present on the GO surface, allow GO structure's chemical modification, thereby affording efficient corrosion inhibitors. While the nanomaterial-based coatings are reported most for the neutral and saline media, the modified GO-based corrosion inhibitors have been reported for aggressive environments, such as 1 M HCl and 15% HCl, and even at elevated temperatures. Recently, CDs have also been explored as inhibitors for aqueous corrosive environments (Fig. 11c). The following section provides some of the literature reports available on green CDs-based corrosion inhibitors. Herein, we have chosen the examples of CDs-based inhibitors focusing on MW, US synthesized methods or using green precursors.

Table 8 provides a comparison of the inhibition performance of some green CDs-based inhibitors. 4-Aminosalicylic acid (ASA), an antibiotic primarily used for tuberculosis treatment, has been considerably reported for the synthesis of CDs following the solvothermal approach. Figure 13a shows the reaction schemes for the preparation of CDs using ASA as the precursor along with some amino acids. The synthesized CDs were N-doped and evaluated as corrosion inhibitors for copper in 0.5 M H_2SO_4 [173], Q235 carbon steel in 1 M HCl [174], and carbon steel in CO_2 saturated 3.5% NaCl [175]. High efficiencies were obtained in a concentration range from 50 to 100 mg L^{-1}. The adsorption of the CDs on the copper and Q235 steel substrates was in agreement with the Langmuir model with a mixed mode of physical and chemical adsorptions. For the carbon steel in a sweet corrosion environment,

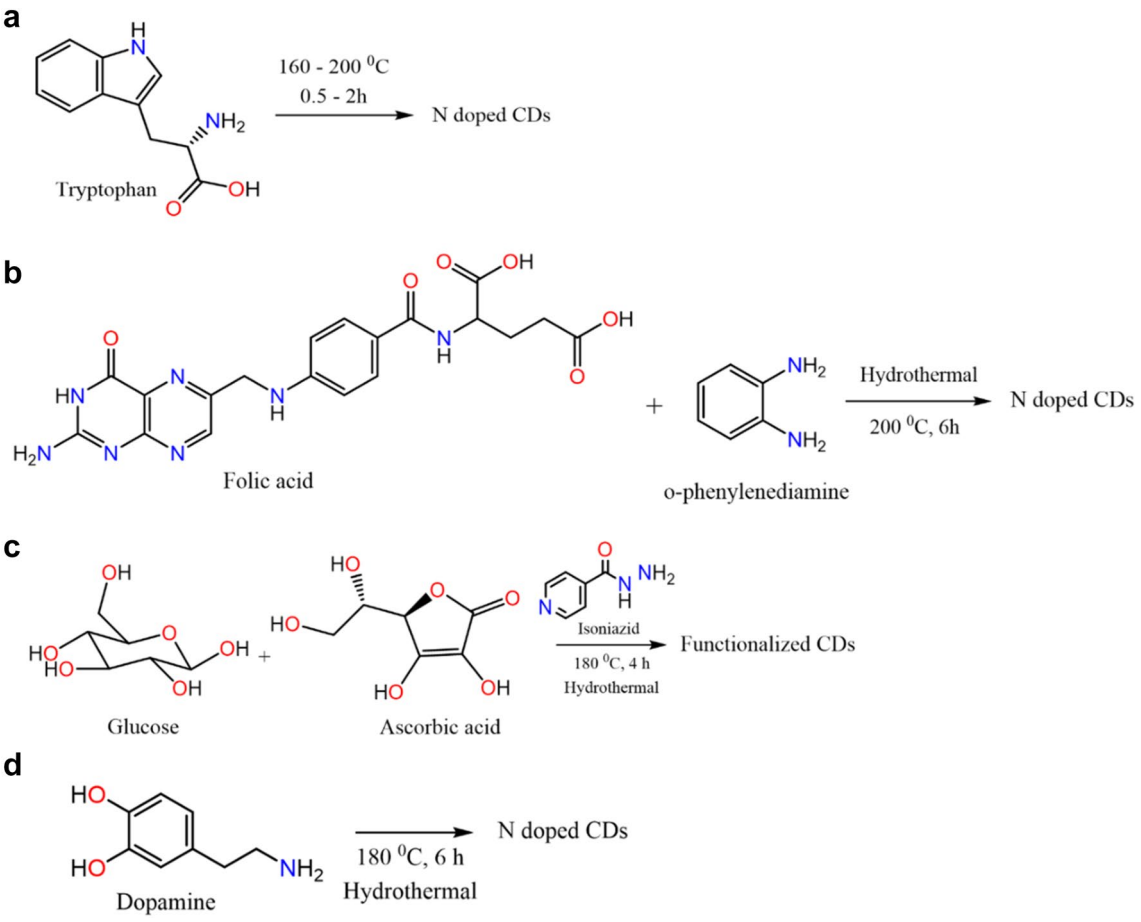

Fig. 14 Schemes for the synthesis of CDs employing **a** tryptophan [181], **b** folic acid [182], **c** glucose, ascorbic acid [183], and **d** dopamine [184] as precursors

the authors compared ASA with the CDs. It was revealed that CDs showed better performance and made the metallic substrate more hydrophobic in comparison to that of ASA alone.

In another study, ASA was used along with L-histidine to afford N-doped CDs that were evaluated for Q235 steel surface in 1 M HCl solution [176]. Weight loss tests, electrochemical corrosion evaluation, and surface analysis supported strong adsorption of the N-CDs on the metal surface. Figure 13b shows the schematic of preparing CDs using citric acid and other precursors. Citric acid is often reported as a green precursor for the synthesis of CDs, alone and in combination with other reagents. Citric acid and L-histidine were used as precursors to obtain N-doped CDs [177]. The CDs showed effective corrosion inhibition with > 90% protection at 100 mg L^{-1}. The studies on density functional theory (DFT) and molecular dynamics (MD) simulations evidenced a low energy gap and high binding energy of the inhibitor. L-Serine and citric acid were used in a solvothermal protocol to afford N-doped CDs [178]. The synthesized nanomaterial was used as an inhibitor against the corrosion of copper using electrochemical, surface, and spectroscopic analyses. High efficiency of 98.5% was afforded after an immersion time of 24 h. An imidazole-based ionic liquid was used to functionalize citric acid-derived CDs to obtain a green corrosion inhibitor for carbon steel surface in 1 M HCl and 3.5% NaCl [179]. The inhibitor showed adherence to Langmuir adsorption isotherm in both cases and followed the physicochemical mode of adsorption.

Using tryptophan as a precursor, a series of N-doped CDs were obtained (Fig. 14a) depending on varying hydrothermal reaction conditions [181]. The developed CDs were used as inhibitors for carbon steel corrosion in 1 M HCl, and high efficiency was obtained at 200 mg L^{-1}. Both physical and chemical adsorption of the CDs was observed on the metallic substrate. Using folic acid and o-phenylenediamine, N-doped CDs were prepared (Fig. 14b) and used as an inhibitor for Q235 steel surface in 1 M HCl solution [182]. High efficiency of 95.4% was obtained in accordance with Langmuir isotherm with a mixed mode of physical and chemical adsorption. Heterocyclic molecules, especially triazole derivatives, have shown considerable adsorption and protection performance for copper metal. Considering this fact, CDs were prepared using glucose, ascorbic acid, and a triazole derivative (Fig. 14c) to afford triazole-modified CDs [183]. The CDs were employed as inhibitors for Cu substrate in 3.5% NaCl using electrochemical techniques and surface examination, wherein a high protection of 88% at 70 mg L^{-1} was obtained.

N, and S-doped, blue-emitting CDs were obtained using citric acid, isoniazid, and thiourea as precursor molecules following a hydrothermal reaction [180]. The material showed efficient performance in 15% HCl on mild steel with > 98% protection after a 6 h immersion period. After prolonged exposure to corrosive media of 48 h, still, high efficiency of > 91% was achieved. CDs derived from *Coffea caneophora* and urea after the pyrolysis procedure was used for Cu corrosion inhibition in 1% NaCl and showed high protection performance [185]. Dopamine was used as a green precursor to afford N-doped CDs (Fig. 14d) that were utilized for the protection of Q235 steel surface in 1 M HCl solution [184]. Even after prolonged exposure of 60 h, a high extent of protection with > 92% efficiency was achieved, which remained almost unchanged even at the elevated temperature of 328 K. Blue-emitting CDs were obtained using durian juice as the precursor, which contained C=O, O–H, and S=O functional groups [186]. The CDs showed strong EIPL with moderate QY. When evaluated for copper in 1% NaCl solution, high protection of 86% was afforded at 800 mg L^{-1}.

7 Conclusions and outlook

This review presents a brief introduction to the significance of CDs with attention focused on the sustainable sources and methodologies for their synthesis. Special emphasis is given to microwave (MW) and ultrasonic (US) irradiation as modern synthetic techniques in compliance with the green chemistry principles. The basic principles governing the organic transformations based on MW and US techniques are described in this report. In comparison to the conventional heating of the reaction mixture using hot plate stirring as well as solvent refluxing, the nanomaterials can be more efficiently produced using MW and US heating with significantly high yield and selectivity. The MW and US heating offer environmentally benign and quicker methods to develop uniform size CDs with scalable yield, and precise control over physicochemical properties. A brief review of literature on the MW- and US-based synthesis of CDs is provided while discussing the important properties such as size, photoluminescence behavior (excitation dependence/independence), emission color, and the quantum yield of the CDs. The major mechanisms of luminescence of CDs are briefly discussed. The significance of green precursors in the production of CDs is given. Some examples of the green precursor-derived CDs is highlighted, e.g., carbohydrates, amino acids, proteins, ionic liquids, and pharmaceutical products. It is shown that using these precursors, the obtained CDs can be doped with N, and S-heteroatoms, heterocycles, and ionic liquid moieties, with high hydrophilicity and biocompatibility.

Some of the major applications of the CDs are also highlighted in the present review. In general, most of the reports focus on LEDs, electrocatalysis, solar cells, antibacterial activity, anticancer activity, sensors, photocatalysis, etc. In addition to the above, in recent years, there have been several

reports on the application of CDs as corrosion inhibitors. Generally, carbon-based nanomaterials such as graphene and graphene oxide have been applied as materials of choice for anti-corrosion coatings and corrosion inhibition. Due to high aqueous solubility, the CDs-based inhibitors can potentially be used as a synergistic component to develop commercial corrosion inhibitor formulations. The utilization of green CDs as corrosion inhibitors is likely to address the issues of toxicity and harmful discharges posed by conventional corrosion inhibitors. It is shown that the CDs display high inhibition performance at a considerably low inhibitor dose and at long exposure times.

Supplementary Information The online version contains supplementary material available at https://doi.org/10.1007/s42823-022-00359-1.

Declarations

Conflict of interest The authors declare that they have no known competing financial interests or personal relationships that could have appeared to influence the work reported in this paper.

References

1. Chauhan DS, Quraishi M, Ansari K, Saleh TA (2020) Graphene and graphene oxide as new class of materials for corrosion control and protection: present status and future scenario. Prog Org Coat 147:105741
2. Georgakilas V, Perman JA, Tucek J, Zboril R (2015) Broad family of carbon nanoallotropes: classification, chemistry, and applications of fullerenes, carbon dots, nanotubes, graphene, nanodiamonds, and combined superstructures. Chem Rev 115:4744–4822
3. Wang Y, Hu A (2014) Carbon quantum dots: synthesis, properties and applications. J Mater Chem C 2:6921–6939
4. Baig N, Sajid M, Saleh TA (2019) Recent trends in nanomaterial-modified electrodes for electroanalytical applications. TrAC Trends Anal Chem 111:47–61
5. Li J, Zhang L, Li P, Zhang Y, Dong C (2018) One step hydrothermal synthesis of carbon nanodots to realize the fluorescence detection of picric acid in real samples. Sens Actuators B Chem 258:580–588
6. Zuo P, Lu X, Sun Z, Guo Y, He H (2016) A review on syntheses, properties, characterization and bioanalytical applications of fluorescent carbon dots. Microchim Acta 183:519–542
7. Kang Z, Lee S-T (2019) Carbon dots: advances in nanocarbon applications. Nanoscale 11:19214–19224
8. Xu X, Ray R, Gu Y, Ploehn HJ, Gearheart L, Raker K, Scrivens WA (2004) Electrophoretic analysis and purification of fluorescent single-walled carbon nanotube fragments. J Am Chem Soc 126:12736–12737
9. Sharma A, Das J (2019) Small molecules derived carbon dots: synthesis and applications in sensing, catalysis, imaging, and biomedicine. J Nanobiotechnol 17:1–24
10. Liu ML, Chen BB, Li CM, Huang CZ (2019) Carbon dots: synthesis, formation mechanism, fluorescence origin and sensing applications. Green Chem 21:449–471
11. Ehtesabi H, Hallaji Z, NajafiNobar S, Bagheri Z (2020) Carbon dots with pH-responsive fluorescence: a review on synthesis and cell biological applications. Microchim Acta 187:1–18
12. de Medeiros TV, Manioudakis J, Noun F, Macairan J-R, Victoria F, Naccache R (2019) Microwave-assisted synthesis of carbon dots and their applications. J Mater Chem C 7:7175–7195
13. Anastas P, Eghbali N (2010) Green chemistry: principles and practice. Chem Soc Rev 39:301–312
14. Kumar R, Kumar VB, Gedanken A (2020) Sonochemical synthesis of carbon dots, mechanism, effect of parameters, and catalytic, energy, biomedical and tissue engineering applications. Ultrason Sonochem 64:105009
15. Cintas P, Luche J-L (1999) Green chemistry. The sonochemical approach. Green Chem 1:115–125
16. Romero MP, Alves F, Stringasci MD, Buzzá HH, Ciol H, Inada NM, Bagnato VS (2021) One-pot microwave-assisted synthesis of carbon dots and in vivo and in vitro antimicrobial photodynamic applications. Front Microbiol 12:1455
17. Kumar VB, Z.e. Porat, A. Gedanken, (2016) Facile one-step sonochemical synthesis of ultrafine and stable fluorescent C-dots. Ultrason Sonochem 28:367–375
18. Saleem M, Naz M, Shukrullah S, Shujah M, Akhtar M, Ullah S, Ali S (2021) One-pot sonochemical preparation of carbon dots, influence of process parameters and potential applications: a review. Carbon Lett 32:1–17
19. Ng HM, Lim G, Leo C (2021) Comparison between hydrothermal and microwave-assisted synthesis of carbon dots from biowaste and chemical for heavy metal detection: a review. Microchem J 165:106116
20. Xia C, Zhu S, Feng T, Yang M, Yang B (2019) Evolution and synthesis of carbon dots: from carbon dots to carbonized polymer dots. Adv Sci 6:1901316
21. Quraishi MA, Chauhan DS, Saji VS (2020) Heterocyclic organic corrosion inhibitors: principles and applications. Elsevier, Amsterdam
22. Moseley JD, Kappe CO (2011) A critical assessment of the greenness and energy efficiency of microwave-assisted organic synthesis. Green Chem 13:794–806
23. Chauhan DS, Gopal CSA, Kumar D, Mahato N, Quraishi MA, Cho MH (2018) Microwave induced facile synthesis and characterization of ZnO nanoparticles as efficient antibacterial agents. Mater Discov 11:19–25
24. Singh P, Chauhan DS, Chauhan SS, Singh G, Quraishi MA (2019) Bioinspired synergistic formulation from dihydropyrimdinones and iodide ions for corrosion inhibition of carbon steel in sulphuric acid. J Mol Liq 298:112051
25. Kappe CO (2004) Controlled microwave heating in modern organic synthesis. Angew Chem Int Ed 43:6250–6284
26. Polshettiwar V, Varma RS (2008) Microwave-assisted organic synthesis and transformations using benign reaction media. Acc Chem Res 41:629–639
27. Tierney J, Lidström P (2009) Microwave assisted organic synthesis. Wiley, Hoboken
28. Chauhan DS, Mazumder MJ, Quraishi MA, Ansari K, Suleiman R (2020) Microwave-assisted synthesis of a new piperonal-chitosan Schiff base as a bio-inspired corrosion inhibitor for oil-well acidizing. Int J Biol Macromol 158:231–243
29. Chauhan DS, Mazumder MJ, Quraishi MA, Ansari K (2020) Chitosan-cinnamaldehyde Schiff base: a bioinspired

macromolecule as corrosion inhibitor for oil and gas industry. Int J Biol Macromol 158:127–138
30. Kappe CO (2008) Microwave dielectric heating in synthetic organic chemistry. Chem Soc Rev 37:1127–1139
31. Yang P, Zhu Z, Zhang W, Zhang T, Li X, Luo M, Chen W, Chen M, Zhou X (2020) Fluorescence mechanism of xylan-derived carbon dots: toward investigation on excitation-related emission behaviors. J Lumin 223:117199
32. He G, Shu M, Yang Z, Ma Y, Huang D, Xu S, Wang Y, Hu N, Zhang Y, Xu L (2017) Microwave formation and photoluminescence mechanisms of multi-states nitrogen doped carbon dots. Appl Surf Sci 422:257–265
33. Yang P, Zhu Z, Zhang T, Chen M, Cao Y, Zhang W, Wang X, Zhou X, Chen W (2019) Facile synthesis and photoluminescence mechanism of green emitting xylose-derived carbon dots for anti-counterfeit printing. Carbon 146:636–649
34. Wang X, Qu K, Xu B, Ren J, Qu X (2011) Microwave assisted one-step green synthesis of cell-permeable multicolor photoluminescent carbon dots without surface passivation reagents. J Mater Chem 21:2445–2450
35. Penteado F, Monti B, Sancineto L, Perin G, Jacob RG, Santi C, Lenardão EJ (2018) Ultrasound-assisted multicomponent reactions, organometallic and organochalcogen chemistry. Asian Org Chem 7:2368–2385
36. Kimura T (2015) Application of ultrasound to organic synthesis. In: Sonochemistry and the acoustic bubble, Elsevier, Amsterdam, p 171–186
37. Li C, Sun X, Li Y, Liu H, Long B, Xie D, Chen J, Wang K (2021) Rapid and green fabrication of carbon dots for cellular imaging and anti-counterfeiting applications. ACS Omega 6:3232–3237
38. Costas-Mora I, Romero V, Lavilla I, Bendicho C (2014) In situ building of a nanoprobe based on fluorescent carbon dots for methylmercury detection. Anal Chem 86:4536–4543
39. Dehvari K, Liu KY, Tseng P-J, Gedda G, Girma WM, Chang J-Y (2019) Sonochemical-assisted green synthesis of nitrogen-doped carbon dots from crab shell as targeted nanoprobes for cell imaging. J Taiwan Inst Chem Eng 95:495–503
40. Verma C, Quraishi MA, Ebenso EE (2018) Microwave and ultrasound irradiations for the synthesis of environmentally sustainable corrosion inhibitors: an overview. Sustain Chem Phar 10:134–147
41. Yang H, Li H, Zhai J, Sun L, Yu H (2014) Simple synthesis of graphene oxide using ultrasonic cleaner from expanded graphite. Ind Eng Chem Res 53:17878–17883
42. Kurian M, Paul A (2021) Recent trends in the use of green sources for carbon dot synthesis—a short review. Carbon Trends 3:100032
43. Chaubey N, Qurashi A, Chauhan DS, Quraishi M (2020) Frontiers and advances in green and sustainable inhibitors for corrosion applications: a critical review. J Mol Liq 321:114385
44. El Mouaden K, El Ibrahimi B, Oukhrib R, Bazzi L, Hammouti B, Jbara O, Tara A, Chauhan DS, Quraishi MA (2018) Chitosan polymer as a green corrosion inhibitor for copper in sulfide-containing synthetic seawater. Int J Biol Macromol 119:1311–1323
45. Mouaden KE, Chauhan DS, Quraishi M, Bazzi L, Hilali M (2020) Cinnamaldehyde-modified chitosan as a bio-derived corrosion inhibitor for acid pickling of copper: microwave synthesis, experimental and computational study. Int J Biol Macromol 164:3709–3717
46. Chauhan DS, Quraishi M, Srivastava V, Haque J, El Ibrahimi B (2021) Virgin and chemically functionalized amino acids as green corrosion inhibitors: influence of molecular structure through experimental and in silico studies. J Mol Struct 1226:129259
47. Quraishi MA, Chauhan DS, Saji VS (2021) Heterocyclic biomolecules as green corrosion inhibitors. J Mol Liq 341:117265
48. Ding H, Yu S-B, Wei J-S, Xiong H-M (2016) Full-color light-emitting carbon dots with a surface-state-controlled luminescence mechanism. ACS Nano 10:484–491
49. Kim S, Hwang SW, Kim M-K, Shin DY, Shin DH, Kim CO, Yang SB, Park JH, Hwang E, Choi S-H (2012) Anomalous behaviors of visible luminescence from graphene quantum dots: interplay between size and shape. ACS Nano 6:8203–8208
50. Bao L, Zhang ZL, Tian ZQ, Zhang L, Liu C, Lin Y, Qi B, Pang DW (2011) Electrochemical tuning of luminescent carbon nanodots: from preparation to luminescence mechanism. Adv Mater 23:5801–5806
51. Yan X, Li B, Li L-S (2013) Colloidal graphene quantum dots with well-defined structures. Acc Chem Res 46:2254–2262
52. Essner JB, Kist JA, Polo-Parada L, Baker GA (2018) Artifacts and errors associated with the ubiquitous presence of fluorescent impurities in carbon nanodots. Chem Mater 30:1878–1887
53. Zhao B, Tan ZA (2021) Fluorescent carbon dots: fantastic electroluminescent materials for light-emitting diodes. Adv Sci 8:2001977
54. Wang F, Chen Y-H, Liu C-Y, Ma D-G (2011) White light-emitting devices based on carbon dots' electroluminescence. Chem Commun 47:3502–3504
55. Paulo-Mirasol S, Martínez-Ferrero E, Palomares E (2019) Direct white light emission from carbon nanodots (C-dots) in solution processed light emitting diodes. Nanoscale 11:11315–11321
56. Alam MB, Yadav K, Shukla D, Srivastava R, Lahiri J, Parmar AS (2019) Carbon quantum dot as electron transporting layer in organic light emitting diode. ChemistrySelect 4:7450–7454
57. Liu X, Zheng J, Yang Y, Chen Y, Liu X (2018) Preparation of N-doped carbon dots based on starch and their application in white LED. Opt Mater 86:530–536
58. Khan WU, Wang D, Wang Y (2018) Highly green emissive nitrogen-doped carbon dots with excellent thermal stability for bioimaging and solid-state LED. Inorg Chem 57:15229–15239
59. Yuan F, Wang Z, Li X, Li Y, Tan ZA, Fan L, Yang S (2017) Bright multicolor bandgap fluorescent carbon quantum dots for electroluminescent light-emitting diodes. Adv Mater 29:1604436
60. Gao N, Huang L, Li T, Song J, Hu H, Liu Y, Ramakrishna S (2020) Application of carbon dots in dye-sensitized solar cells: a review. J Appl Polym Sci 137:48443
61. Luo H, Guo Q, Szilágyi PÁ, Jorge AB, Titirici M-M (2020) Carbon dots in solar-to-hydrogen conversion. Trends Chem 2:623–637
62. Feng T, Tao S, Yue D, Zeng Q, Chen W, Yang B (2020) Recent advances in energy conversion applications of carbon dots: from optoelectronic devices to electrocatalysis. Small 16:2001295
63. Gupta V, Chaudhary N, Srivastava R, Sharma GD, Bhardwaj R, Chand S (2011) Luminscent graphene quantum dots for organic photovoltaic devices. J Am Chem Soc 133:9960–9963
64. Kwon W, Lee G, Do S, Joo T, Rhee SW (2014) Size-controlled soft-template synthesis of carbon nanodots toward versatile photoactive materials. Small 10:506–513
65. Sharma V, Jha PK (2019) Enhancement in power conversion efficiency of edge-functionalized graphene quantum dot through adatoms for solar cell applications. Sol Energy Mater Sol Cells 200:109908
66. Hasan MT, Gonzalez-Rodriguez R, Ryan C, Pota K, Green K, Coffer JL, Naumov AV (2019) Nitrogen-doped graphene

quantum dots: optical properties modification and photovoltaic applications. Nano Res 12:1041–1047
67. Briscoe J, Marinovic A, Sevilla M, Dunn S, Titirici M (2015) Biomass-derived carbon quantum dot sensitizers for solid-state nanostructured solar cells. Angew Chem Int Ed 54:4463–4468
68. Wang H, Sun P, Cong S, Wu J, Gao L, Wang Y, Dai X, Yi Q, Zou G (2016) Nitrogen-doped carbon dots for "green" quantum dot solar cells. Nanoscale Res Lett 11:1–6
69. Zhang Q, Zhang G, Sun X, Yin K, Li H (2017) Improving the power conversion efficiency of carbon quantum dot-sensitized solar cells by growing the dots on a TiO_2 photoanode in situ. Nanomaterials 7:130
70. Zhao Y, Duan J, He B, Jiao Z, Tang Q (2018) Improved charge extraction with N-doped carbon quantum dots in dye-sensitized solar cells. Electrochim Acta 282:255–262
71. Zhu W, Duan J, Duan Y, Zhao Y, Tang Q (2017) Efficiency enhancement of hybridized solar cells through co-sensitization and fast charge extraction by up-converted polyethylene glycol modified carbon quantum dots. J Power Sources 367:158–166
72. Lv K, Suo W, Shao M, Zhu Y, Wang X, Feng J, Fang M (2019) Nitrogen doped MoS_2 and nitrogen doped carbon dots composite catalyst for electroreduction CO_2 to CO with high Faradaic efficiency. Nano Energy 63:103834
73. Li W, Liu Y, Wu M, Feng X, Redfern SA, Shang Y, Yong X, Feng T, Wu K, Liu Z (2018) Carbon-quantum-dots-loaded ruthenium nanoparticles as an efficient electrocatalyst for hydrogen production in alkaline media. Adv Mater 30:1800676
74. Xie Z, Yu S, Fan X-B, Wei S, Yu L, Zhong Y, Gao X-W, Wu F, Zhou Y (2021) Wavelength-sensitive photocatalytic H_2 evolution from H_2S splitting over g-C3N4 with S, N-codoped carbon dots as the photosensitizer. J Energy Chem 52:234–242
75. Cheng R, Chung C-C, Wang S, Cao B, Zhang M, Chen C, Wang Z, Chen M, Shen S, Feng S-P (2021) Three-dimensional self-attaching perovskite quantum dots/polymer platform for efficient solar-driven CO_2 reduction. Mater Today Phys 17:100358
76. Xu Y, Yu H, Chudal L, Pandey NK, Amador EH, Bui B, Wang L, Ma X, Deng S, Zhu X (2021) Striking luminescence phenomena of carbon dots and their applications as a double ratiometric fluorescence probes for H_2S detection. Mater Today Phys 17:100328
77. Tian L, Li Z, Wang P, Zhai X, Wang X, Li T (2021) Carbon quantum dots for advanced electrocatalysis. J Energy Chem 55:279–294
78. Zhao Z, Zhang H, Song X, Shi Y, Si D, Li H, Hao C (2021) Insight into the CO_2 photoreduction mechanism over 9-hydroxyphenal-1-one (HPHN) carbon quantum dots. J Energy Chem 52:269–276
79. Yuan J, Rujisamphan N, Ma W, Yuan J, Li Y, Lee S-T (2021) Perspective on the perovskite quantum dots for flexible photovoltaics. J Energy Chem 62:505–507
80. Bhattacharyya S, Konkena B, Jayaramulu K, Schuhmann W, Maji TK (2017) Synthesis of nano-porous carbon and nitrogen doped carbon dots from an anionic MOF: a trace cobalt metal residue in carbon dots promotes electrocatalytic ORR activity. J Mater Chem A 5:13573–13580
81. Shin J, Guo J, Zhao T, Guo Z (2019) Functionalized carbon dots on graphene as outstanding non-metal bifunctional oxygen electrocatalyst. Small 15:1900296
82. Zhang J, Chen J, Luo Y, Chen Y, Wei X, Wang G, Wang R (2019) Sandwich-like electrode with tungsten nitride nanosheets decorated with carbon dots as efficient electrocatalyst for oxygen reduction. Appl Surf Sci 466:911–919
83. Zhang P, Bin D, Wei J-S, Niu X-Q, Chen X-B, Xia Y-Y, Xiong H-M (2019) Efficient oxygen electrocatalyst for Zn–air batteries: carbon dots and Co9S8 nanoparticles in a N, S-codoped carbon matrix. ACS Appl Mater Interfaces 11:14085–14094
84. Feng T, Zeng Q, Lu S, Yang M, Tao S, Chen Y, Zhao Y, Yang B (2019) Morphological and interfacial engineering of cobalt-based electrocatalysts by carbon dots for enhanced water splitting. ACS Sustain Chem Eng 7:7047–7057
85. Gao S, Chen Y, Fan H, Wei X, Hu C, Wang L, Qu L (2014) A green one-arrow-two-hawks strategy for nitrogen-doped carbon dots as fluorescent ink and oxygen reduction electrocatalysts. J Mater Chem A 2:6320–6325
86. Liu Y, Li Z, Green M, Just M, Li YY, Chen X (2017) Titanium dioxide nanomaterials for photocatalysis. J Phys D Appl Phys 50:193003
87. Han M, Zhu S, Lu S, Song Y, Feng T, Tao S, Liu J, Yang B (2018) Recent progress on the photocatalysis of carbon dots: classification, mechanism and applications. Nano Today 19:201–218
88. Yao Y, Zhang H, Hu K, Nie G, Yang Y, Wang Y, Duan X, Wang S (2022) Carbon dots based photocatalysis for environmental applications. J Environ Chem Eng 10:107336
89. Zhang Z, Yi G, Li P, Zhang X, Fan H, Zhang Y, Wang X, Zhang C (2020) A minireview on doped carbon dots for photocatalytic and electrocatalytic applications. Nanoscale 12:13899–13906
90. Jusuf BN, Sambudi NS, Samsuri S (2018) Microwave-assisted synthesis of carbon dots from eggshell membrane ashes by using sodium hydroxide and their usage for degradation of methylene blue. J Environ Chem Eng 6:7426–7433
91. Li Y, Zhang B-P, Zhao J-X, Ge Z-H, Zhao X-K, Zou L (2013) ZnO/carbon quantum dots heterostructure with enhanced photocatalytic properties. Appl Surf Sci 279:367–373
92. Kumar VB, Perelshtein I, Lipovsky A, Porat ZE, Gedanken A (2015) The sonochemical synthesis of Ga@ C-dots particles. RSC Adv 5:25533–25540
93. Hu Y, Li M, Gao Z, Wang L, Zhang J (2021) Waste polyethylene terephthalate derived carbon dots for separable production of 5-hydroxymethylfurfural at low temperature. Catal Lett 151:2436–2444
94. Pham-Truong T-N, Petenzi T, Ranjan C, Randriamahazaka H, Ghilane J (2018) Microwave assisted synthesis of carbon dots in ionic liquid as metal free catalyst for highly selective production of hydrogen peroxide. Carbon 130:544–552
95. Chen J, Fan T, Xie Z, Zeng Q, Xue P, Zheng T, Chen Y, Luo X, Zhang H (2020) Advances in nanomaterials for photodynamic therapy applications: status and challenges. Biomaterials 237:119827
96. Fan H-Y, Yu X-H, Wang K, Yin Y-J, Tang Y-J, Tang Y-L, Liang X-H (2019) Graphene quantum dots (GQDs)-based nanomaterials for improving photodynamic therapy in cancer treatment. Eur J Med Chem 182:111620
97. Day RA, Sletten EM (2021) Perfluorocarbon nanomaterials for photodynamic therapy. Curr Opin Colloid Interface Sci 54:101454
98. Dolmans DE, Fukumura D, Jain RK (2003) Photodynamic therapy for cancer. Nat Rev Cancer 3:380–387
99. Zhang D-Y, Zheng Y, Zhang H, He L, Tan C-P, Sun J-H, Zhang W, Peng X, Zhan Q, Ji L-N (2017) Ruthenium complex-modified carbon nanodots for lysosome-targeted one-and two-photon imaging and photodynamic therapy. Nanoscale 9:18966–18976
100. Jhonsi MA, Ananth DA, Nambirajan G, Sivasudha T, Yamini R, Bera S, Kathiravan A (2018) Antimicrobial activity, cytotoxicity and DNA binding studies of carbon dots. Spectrochim Acta Part A Mol Biomol Spectrosc 196:295–302

101. Dong X, Liang W, Meziani MJ, Sun Y-P, Yang L (2020) Carbon dots as potent antimicrobial agents. Theranostics 10:671
102. Choi Y, Kim S, Choi MH, Ryoo SR, Park J, Min DH, Kim BS (2014) Highly biocompatible carbon nanodots for simultaneous bioimaging and targeted photodynamic therapy in vitro and in vivo. Adv Func Mater 24:5781–5789
103. Bao X, Yuan Y, Chen J, Zhang B, Li D, Zhou D, Jing P, Xu G, Wang Y, Holá K (2018) In vivo theranostics with near-infrared-emitting carbon dots—highly efficient photothermal therapy based on passive targeting after intravenous administration. Light Sci Appl 7:1–11
104. Raina S, Thakur A, Sharma A, Pooja D, Minhas AP (2020) Bactericidal activity of *Cannabis sativa* phytochemicals from leaf extract and their derived carbon dots and Ag@ carbon dots. Mater Lett 262:127122
105. Liu J, Lu S, Tang Q, Zhang K, Yu W, Sun H, Yang B (2017) One-step hydrothermal synthesis of photoluminescent carbon nanodots with selective antibacterial activity against *Porphyromonas gingivalis*. Nanoscale 9:7135–7142
106. John TS, Yadav PK, Kumar D, Singh SK, Hasan SH (2020) Highly fluorescent carbon dots from wheat bran as a novel drug delivery system for bacterial inhibition. Luminescence 35:913–923
107. Sahiner N, Suner SS, Sahiner M, Silan C (2019) Nitrogen and sulfur doped carbon dots from amino acids for potential biomedical applications. J Fluoresc 29:1191–1200
108. Lin J, Huang Y, Huang P (2018) Graphene-based nanomaterials in bioimaging. In: Biomedical applications of functionalized nanomaterials, vol 105, no (Pt B), pp 247–287
109. Schnermann MJ (2017) Organic dyes for deep bioimaging. Nature 551:176–177
110. Kim D, Kim J, Park YI, Lee N, Hyeon T (2018) Recent development of inorganic nanoparticles for biomedical imaging. ACS Cent Sci 4:324–336
111. Martynenko I, Litvin A, Purcell-Milton F, Baranov A, Fedorov A, Gun'Ko Y (2017) Application of semiconductor quantum dots in bioimaging and biosensing. J Mater Chem B 5:6701–6727
112. Li H, Yan X, Kong D, Jin R, Sun C, Du D, Lin Y, Lu G (2020) Recent advances in carbon dots for bioimaging applications. Nanoscale Horiz 5:218–234
113. Cao L, Wang X, Meziani MJ, Lu F, Wang H, Luo PG, Lin Y, Harruff BA, Veca LM, Murray D (2007) Carbon dots for multiphoton bioimaging. J Am Chem Soc 129:11318–11319
114. Zheng M, Liu S, Li J, Xie Z, Qu D, Miao X, Jing X, Sun Z, Fan H (2015) Preparation of highly luminescent and color tunable carbon nanodots under visible light excitation for in vitro and in vivo bio-imaging. J Mater Res 30:3386–3393
115. Naik GG, Alam MB, Pandey V, Mohapatra D, Dubey PK, Parmar AS, Sahu AN (2020) Multi-Functional carbon dots from an ayurvedic medicinal plant for cancer cell bioimaging applications. J Fluoresc 30:407–418
116. Amjad M, Iqbal M, Faisal A, Junjua AM, Hussain I, Hussain SZ, Ghramh HA, Khan KA, Janjua HA (2019) Hydrothermal synthesis of carbon nanodots from bovine gelatin and PHM3 microalgae strain for anticancer and bioimaging applications. Nanoscale Adv 1:2924–2936
117. Wang D, Zhu L, Mccleese C, Burda C, Chen J-F, Dai L (2016) Fluorescent carbon dots from milk by microwave cooking. RSC Adv 6:41516–41521
118. Liu Y, Xiao N, Gong N, Wang H, Shi X, Gu W, Ye L (2014) One-step microwave-assisted polyol synthesis of green luminescent carbon dots as optical nanoprobes. Carbon 68:258–264
119. Pan L, Sun S, Zhang L, Jiang K, Lin H (2016) Near-infrared emissive carbon dots for two-photon fluorescence bioimaging. Nanoscale 8:17350–17356
120. Teodoro KB, Sanfelice RC, Migliorini FL, Pavinatto A, Facure MH, Correa DS (2021) A review on the role and performance of cellulose nanomaterials in sensors. ACS Sens 6:2473–2496
121. Saha K, Agasti SS, Kim C, Li X, Rotello VM (2012) Gold nanoparticles in chemical and biological sensing. Chem Rev 112:2739–2779
122. Sun X, Lei Y (2017) Fluorescent carbon dots and their sensing applications. TrAC Trends Anal Chem 89:163–180
123. Junaid HM, Solangi AR, Batool M (2021) Carbon dots as naked eye sensors. Analyst 146:2463–2474
124. Lin X, Xiong M, Zhang J, He C, Ma X, Zhang H, Kuang Y, Yang M, Huang Q (2021) Carbon dots based on natural resources: Synthesis and applications in sensors. Microchem J 160:105604
125. Liu Q, Zhang N, Shi H, Ji W, Guo X, Yuan W, Hu Q (2018) One-step microwave synthesis of carbon dots for highly sensitive and selective detection of copper ions in aqueous solution. New J Chem 42:3097–3101
126. López C, Zougagh M, Algarra M, Rodríguez-Castellón E, Campos B, Da Silva JE, Jiménez-Jiménez J, Ríos A (2015) Microwave-assisted synthesis of carbon dots and its potential as analysis of four heterocyclic aromatic amines. Talanta 132:845–850
127. Xu Z, Wang C, Jiang K, Lin H, Huang Y, Zhang C (2015) Microwave-assisted rapid synthesis of amphibious yellow fluorescent carbon dots as a colorimetric nanosensor for Cr(VI). Part Part Syst Charact 32:1058–1062
128. Liu X, Li T, Hou Y, Wu Q, Yi J, Zhang G (2016) Microwave synthesis of carbon dots with multi-response using denatured proteins as carbon source. RSC Adv 6:11711–11718
129. Yang P, Zhu Z, Chen W, Luo M, Zhang W, Zhang T, Chen M, Zhou X (2020) Nitrogen/sulfur Co-doping strategy to synthesis green-yellow emitting carbon dots derived from xylose: toward application in pH sensing. J Lumin 227:117489
130. Ahmadian-Fard-Fini S, Ghanbari D, Amiri O, Salavati-Niasari M (2021) Green sonochemistry assisted synthesis of hollow magnetic and photoluminescent $MgFe_2O_4$–carbon dot nanocomposite as a sensor for toxic Ni(II), Cd(II) and Hg(II) ions and bacteria. RSC Adv 11:22805–22811
131. Cheng W, Xu J, Guo Z, Yang D, Chen X, Yan W, Miao P (2018) Hydrothermal synthesis of N, S co-doped carbon nanodots for highly selective detection of living cancer cells. J Mater Chem B 6:5775–5780
132. Pandit S, Behera P, Sahoo J, De M (2019) In situ synthesis of amino acid functionalized carbon dots with tunable properties and their biological applications. ACS Appl Bio Mater 2:3393–3403
133. Cheng H-J, Kao C-L, Chen Y-F, Huang P-C, Hsu C-Y, Kuei C-H (2017) Amino acid derivatized carbon dots with tunable selectivity as logic gates for fluorescent sensing of metal cations. Microchim Acta 184:3179–3187
134. Yang X, Liu M, Yin Y, Tang F, Xu H, Liao X (2018) Green, hydrothermal synthesis of fluorescent carbon nanodots from gardenia, enabling the detection of metronidazole in pharmaceuticals and rabbit plasma. Sensors 18:964
135. Yadav PK, Singh VK, Chandra S, Bano D, Kumar V, Talat M, Hasan SH (2018) Green synthesis of fluorescent carbon quantum dots from azadirachta indica leaves and their peroxidase-mimetic activity for the detection of H_2O_2 and ascorbic acid in common fresh fruits. ACS Biomater Sci Eng 5:623–632
136. Chandra S, Bano D, Pradhan P, Singh VK, Yadav PK, Sinha D, Hasan SH (2020) Nitrogen/sulfur-co-doped carbon quantum dots: a biocompatible material for the selective detection of picric acid in aqueous solution and living cells. Anal Bioanal Chem 412:3753–3763

137. Singh AK, Singh VK, Singh M, Singh P, Khadim SR, Singh U, Koch B, Hasan S, Asthana R (2019) One pot hydrothermal synthesis of fluorescent NP-carbon dots derived from *Dunaliella salina* biomass and its application in on-off sensing of Hg(II), Cr(VI) and live cell imaging. J Photochem Photobiol A 376:63–72
138. Singh VK, Yadav PK, Chandra S, Bano D, Talat M, Hasan SH (2018) Peroxidase mimetic activity of fluorescent NS-carbon quantum dots and their application in colorimetric detection of H_2O_2 and glutathione in human blood serum. J Mater Chem B 6:5256–5268
139. Chandra S, Bano D, Sahoo K, Kumar D, Kumar V, Yadav PK, Hasan SH (2022) Synthesis of fluorescent carbon quantum dots from Jatropha fruits and their application in fluorometric sensor for the detection of chlorpyrifos. Microchem J 172:106953
140. Bano D, Kumar V, Singh VK, Chandra S, Singh DK, Yadav PK, Talat M, Hasan SH (2018) A facile and simple strategy for the synthesis of label free carbon quantum dots from the latex of *Euphorbia milii* and its peroxidase-mimic activity for the naked eye detection of glutathione in a human blood serum. ACS Sustain Chem Eng 7:1923–1932
141. Chandra S, Singh VK, Yadav PK, Bano D, Kumar V, Pandey VK, Talat M, Hasan SH (2019) Mustard seeds derived fluorescent carbon quantum dots and their peroxidase-like activity for colorimetric detection of H_2O_2 and ascorbic acid in a real sample. Anal Chim Acta 1054:145–156
142. Fontana MG, Greene ND (2018) Corrosion engineering. McGraw-Hill, New York
143. Revie RW (2011) Uhlig's corrosion handbook. Wiley, Hoboken
144. Sastri VS (1998) Corrosion inhibitors: principles and applications. Wiley, Hoboken
145. Sastri VS (2012) Green corrosion inhibitors: theory and practice. Wiley, Hoboken
146. Koch G, Varney J, Thompson N, Moghissi O, Gould M, Payer J (2016) International measures of prevention, application, and economics of corrosion technologies study. NACE International, Houston
147. Geim AK, Novoselov KS (2010) The rise of graphene. In: Rodgers P (ed) Nanoscience and technology: a collection of reviews from nature journals. World Scientific, Singapore, pp 11–19
148. Allen MJ, Tung VC, Kaner RB (2009) Honeycomb carbon: a review of graphene. Chem Rev 110:132–145
149. Singh V, Joung D, Zhai L, Das S, Khondaker SI, Seal S (2011) Graphene based materials: past, present and future. Prog Mater Sci 56:1178–1271
150. Li W, Dong H, Wang L, Li N, Guo X, Li J, Qiu Y (2014) Montmorillonite as bifunctional buffer layer material for hybrid perovskite solar cells with protection from corrosion and retarding recombination. J Mater Chem A 2:13587–13592
151. Wu L, Dong Y, Zhao J, Ma D, Huang W, Zhang Y, Wang Y, Jiang X, Xiang Y, Li J (2019) Kerr nonlinearity in 2D graphdiyne for passive photonic diodes. Adv Mater 31:1807981
152. Singh A, Ansari KR, Chauhan DS, Quraishi MA, Lgaz H, Chung I-M (2020) Comprehensive investigation of steel corrosion inhibition at macro/micro level by ecofriendly green corrosion inhibitor in 15% HCl medium. J Colloid Interface Sci 560:225–236
153. Ansari KR, Quraishi MA, Singh A (2015) Isatin derivatives as a non-toxic corrosion inhibitor for mild steel in 20% H2SO4. Corros Sci 95:62–70
154. Ansari KR, Quraishi MA, Singh A, Ramkumar S, Obote IB (2016) Corrosion inhibition of N80 steel in 15% HCl by pyrazolone derivatives: electrochemical, surface and quantum chemical studies. RSC Adv 6:24130–24141
155. Haque J, Ansari K, Srivastava V, Quraishi MA, Obot I (2017) Pyrimidine derivatives as novel acidizing corrosion inhibitors for N80 steel useful for petroleum industry: a combined experimental and theoretical approach. J Ind Eng Chem 49:176–188
156. Ansari KR, Quraishi MA (2015) Experimental and computational studies of naphthyridine derivatives as corrosion inhibitor for N80 steel in 15% hydrochloric acid. Physica E 69:322–331
157. Chauhan DS, Ansari KR, Sorour AA, Quraishi MA, Lgaz H, Salghi R (2018) Thiosemicarbazide and thiocarbohydrazide functionalized chitosan as ecofriendly corrosion inhibitors for carbon steel in hydrochloric acid solution. Int J Biol Macromol 107:1747–1757
158. Solomon MM, Gerengi H, Kaya T, Umoren SA (2016) Performance evaluation of a chitosan/silver nanoparticles composite on St37 steel corrosion in a 15% HCl solution. ACS Sustain Chem Eng 5:809–820
159. Solomon MM, Gerengi H, Kaya T, Kaya E, Umoren SA (2017) Synergistic inhibition of St37 steel corrosion in 15% H_2SO_4 solution by chitosan and iodide ion additives. Cellulose 24:931–950
160. Solomon MM, Umoren SA, Obot IB, Sorour AA, Gerengi H (2018) Exploration of dextran for application as corrosion inhibitor for steel in strong acid environment: effect of molecular weight, modification, and temperature on efficiency. ACS Appl Mater Interfaces 10:28112–28129
161. Quadri TW, Olasunkanmi LO, Fayemi OE, Solomon MM, Ebenso EE (2017) Zinc oxide nanocomposites of selected polymers: synthesis, characterization, and corrosion inhibition studies on mild steel in HCl solution. ACS Omega 2:8421–8437
162. Gupta RK, Malviya M, Verma C, Quraishi MA (2017) Aminoazobenzene and diaminoazobenzene functionalized graphene oxides as novel class of corrosion inhibitors for mild steel: experimental and DFT studies. Mater Chem Phys 198:360–373
163. Gupta RK, Malviya M, Ansari KR, Lgaz H, Chauhan DS, Quraishi MA (2019) Functionalized graphene oxide as a new generation corrosion inhibitor for industrial pickling process: DFT and experimental approach. Mater Chem Phys 236:121727
164. Gupta RK, Malviya M, Verma C, Gupta NK, Quraishi MA (2017) Pyridine-based functionalized graphene oxides as a new class of corrosion inhibitors for mild steel: an experimental and DFT approach. RSC Adv 7:39063–39074
165. Ansari K, Chauhan DS, Quraishi M, Saleh TA (2020) Surfactant modified graphene oxide as novel corrosion inhibitors for mild steels in acidic media. Inorg Chem Commun 121:108238
166. Baig N, Chauhan DS, Saleh TA, Quraishi MA (2019) Diethylenetriamine functionalized graphene oxide as a novel corrosion inhibitor for mild steel in hydrochloric acid solutions. New J Chem 43:2328–2337
167. Haruna K, Saleh TA, Obot I, Umoren SA (2019) Cyclodextrin-based functionalized graphene oxide as an effective corrosion inhibitor for carbon steel in acidic environment. Prog Org Coat 128:157–167
168. Ansari KR, Chauhan DS, Quraishi MA, Saleh TA (2020) Bis (2-aminoethyl) amine-modified graphene oxide nanoemulsion for carbon steel protection in 15% HCl: Effect of temperature and synergism with iodide ions. J Colloid Interface Sci 564:124–133
169. Ansari K, Chauhan DS, Quraishi MA, Adesina A, Saleh TA (2020) The synergistic influence of polyethyleneimine-grafted graphene oxide and iodide for the protection of steel in acidizing conditions. RSC Adv 10:17739–17751
170. Quraishi MA, Singh Chauhan D, Rahmani Ansari K, Madhan Kumar A, Saleh TA (2021) polyethyleneimine functionalized graphene oxide: a promising inhibitor for corrosion of copper in the hydrochloric acid environment. J Nanosci Nanotechnol 21:3256–3268
171. Sharifi Z, Pakshir M, Amini A, Rafiei R (2019) Hybrid graphene oxide decoration and water-based polymers for mild steel surface protection in saline environment. J Ind Eng Chem 74:41–54

172. Radey HH, Khalaf MN, Al-Sawaad HZ (2018) Novel corrosion inhibitors for carbon steel alloy in acidic medium of 1N HCl Synthesized from graphene oxide. Open J Org Polym Mater 8:53
173. Qiang Y, Zhang S, Zhao H, Tan B, Wang L (2019) Enhanced anticorrosion performance of copper by novel N-doped carbon dots. Corros Sci 161:108193
174. Cui M, Ren S, Xue Q, Zhao H, Wang L (2017) Carbon dots as new eco-friendly and effective corrosion inhibitor. J Alloy Compd 726:680–692
175. Cen H, Chen Z, Guo X (2019) N, S co-doped carbon dots as effective corrosion inhibitor for carbon steel in CO_2-saturated 3.5% NaCl solution. J Taiwan Inst Chem Eng 99:224–238
176. Pan L, Li G, Wang Z, Liu D, Zhu W, Tong C, Zhu R, Hu S (2021) Carbon dots as environment-friendly and efficient corrosion inhibitors for Q235 steel in 1 M HCl. Langmuir 37:14336–14344
177. Ye Y, Zhang D, Zou Y, Zhao H, Chen H (2020) A feasible method to improve the protection ability of metal by functionalized carbon dots as environment-friendly corrosion inhibitor. J Clean Prod 264:121682
178. Zhang Y, Zhang S, Tan B, Guo L, Li H (2021) Solvothermal synthesis of functionalized carbon dots from amino acid as an eco-friendly corrosion inhibitor for copper in sulfuric acid solution. J Colloid Interface Sci 604:1–14
179. Yang D, Ye Y, Su Y, Liu S, Gong D, Zhao H (2019) Functionalization of citric acid-based carbon dots by imidazole toward novel green corrosion inhibitor for carbon steel. J Clean Prod 229:180–192
180. Saraswat V, Yadav M (2021) Improved corrosion resistant performance of mild steel under acid environment by novel carbon dots as green corrosion inhibitor. Colloids Surf A 627:127172
181. Luo J, Cheng X, Zhong C, Chen X, Ye Y, Zhao H, Chen H (2021) Effect of reaction parameters on the corrosion inhibition behavior of N-doped carbon dots for metal in 1 M HCl solution. J Mol Liq 338:116783
182. Zhu M, Guo L, He Z, Marzouki R, Zhang R, Berdimurodov E (2022) Insights into the newly synthesized N-doped carbon dots for Q235 steel corrosion retardation in acidizing media: a detailed multidimensional study. J Colloid Interface Sci 608:2039–2049
183. Wan S, Chen H, Liao B, Guo X (2021) Adsorption and anticorrosion mechanism of glucose-based functionalized carbon dots for copper in neutral solution. J Taiwan Inst Chem Eng 129:289–298
184. Cui M, Yu Y, Zheng Y (2021) Effective corrosion inhibition of carbon steel in hydrochloric acid by dopamine-produced carbon dots. Polymers 13:1923
185. Christopher K, Mas'ud ZA, Hanif N (2019) Versatile coffee carbon dots as lead(II) and copper(II) ion fluorescence detectors and copper corrosion inhibitor. Int J Sci Res Sci Eng Technol 6:129–138
186. Anindita F, Darmawan N, Mas'ud ZA (2018) Fluorescence carbon dots from durian as an eco-friendly inhibitor for copper corrosion. In: AIP conference proceedings, AIP Publishing LLC, p 020008